

Planck's Constant as a Dynamical Field
Rand Dannenberg
Optical Physics Company, Simi Valley, CA
Ventura College, Physics and Astronomy Ventura, CA
rdannenberg@opci.com
rdannenberg@vcccd.edu

January 24, 2019

Abstract. The constant \hbar is elevated to a dynamical field, coupling to other fields, and itself, through the Lagrangian density derivative terms. The spatial and temporal dependence of \hbar falls directly out of the field equations themselves. Three solutions are found: a free field with a tadpole term; a standing-wave non-propagating mode; a non-oscillating non-propagating mode. The first two are quantizable, and the third is not. The third corresponds to a zero-momentum classical field that naturally decays spatially to a constant with no ad-hoc terms added to the Lagrangian. An attempt is made to calibrate the constants in the third solution based on experimental data. The three fields are referred to as actons. It is tentatively concluded that the acton origin coincides with a massive body, or point of infinite density, though is not mass dependent. An expression for the positional dependence of Planck's constant is derived from a field theory in this work that matches in functional form that of one derived from considerations of Local Position Invariance violation in GR in another paper by this author. Astrophysical and Cosmological interpretations are provided.

1. Introduction

At this time, there are three premier problems in physics, that Occam's Razor, as a guiding principle, suggests there is a single explanation for: the nature of dark energy; the nature of dark matter; the nature of fundamental physical constants.

Constants of nature are measured carefully, seem to be only very weakly dependent on position, and if time varying, this time variation must be very slow. A solution is sought that is consistent with those observations that still might explain how a constant can come into being from some sort of field, that can describe energies associated with the constant, and variations with time or position, if any. One must also explain why the constants do not seem to be limited by the need to propagate at a speed c or lower to have an effect – they are infinite in range, everywhere at all times, nearly equal in magnitude in all locations, persistent in duration, operate seemingly without any mechanism, and there are no easily observed particles associated with them. These observations are consistent with the non-propagating modes of fields, or static fields.

The following section is reproduced nearly *verbatim* from the authors own article: "Position Dependent Planck's Constant in a Frequency-Conserving Schrödinger Equation" *Symmetry* **2020**, *12*, 490; doi:10.3390/sym12040490. Some minor alterations in the text include a reordering of the same references, and a renumbering of the equations to be consistent with present article:

“The possibility of the variation of fundamental constants would impact all present physical theory, while all reported variations or interpretations of data concluding a constant has varied are extremely controversial. Examples of work in this area include Dirac’s Large Number Hypotheses [1], the Oklo mine from which could be extracted a variation of the fine structure constant [2,3], and the observations of quasars bounding the variation of the latter per year to one part in 10^{17} [4-6]. Recent theoretical work includes the impact of time dependent stochastic fluctuations of Planck’s constant [7], and the effect of a varying Planck’s constant on mixed quantum states [8]. An authoritative review of the status of the variations of fundamental constants is given in [9].

Publicly available Global Positioning System (GPS) data was used to attempt to confirm the Local Position Invariance (LPI) of Planck’s constant under General Relativity [10-11]. LPI is a concept from General Relativity, where all local non-gravitational experimental results in freely falling reference frames should be independent of the location that the experiment is performed in. That foundational rule should hold when the fundamental physical constants are not dependent on the location. If the fundamental constants vary universally, but their changes are only small locally, then it is the form of the physical laws that should be the same in all locations.

The LPI violation parameter due to variations in Planck’s constant is called β_h . The fractional variation of Planck’s constant is proportional to the gravitational potential difference and β_h . The value found in [10] for variations in Planck’s constant was $|\beta_h| < 0.007$. This parameter is not zero, and is the largest of the violation parameters extracted in the study. The study did not report on the altitude dependence of Planck’s constant above the earth. A very recent study involving the Galileo satellites found that GR could explain the frequency shift of the onboard hydrogen maser clocks to within a factor of $(4.5 \pm 3.1) \times 10^{-5}$ [12], improved over Gravity Probe A in 1976 of $\sim 1.4 \times 10^{-4}$, these are the α_{rs} redshift violation values that may be compared to β_h .

Consistent sinusoidal oscillations in the decay rate of a number of radioactive elements with periods of one year taken over a 20 year span has been reported [13-18]. These measurements were taken by six organizations on three continents. As both the strong and weak forces were involved in the decay processes, and might be explainable by oscillations of \hbar influencing the probability of tunneling, an all electromagnetic experiment was conducted, designed specifically to be sensitive to Planck’s constant variations [19]. Consistent systematic sinusoidal oscillations of the tunneling voltage of Esaki diodes with periods of one year were monitored for 941 days. The charge carrier tunneling of an Esaki diode can be modeled using the Wentzel–Kramers–Brillouin (WKB) approximation. The result is a tunneling probability that is an exponential function of the physical width of the barrier, and the applied voltage. The tunnel diode oscillations were attributed to the combined effect of changes in the WKB tunneling exponent going as \hbar^{-1} , and changes in the width of the barrier going as \hbar^2 . The electromagnetic experiment voltage oscillations were correctly predicted to be 180 degrees out of phase with the radioactive decay oscillations. This data can be made available for independent analysis by requesting it from the author of [19].

It is both controversial, and easily criticized, to suspect that the oscillations of decay rates and tunnel diode voltage are related to the relative position of the sun to the orbiting earth, and that there are resulting oscillations in Planck’s constant due to position dependent gravitational effects, or effects with proximity to the sun. It should be mentioned that there have been studies in which it was concluded there was no gravitational dependence to the decay rate oscillations [20-21]. There is also dispute in the literature concerning the reality of the decay rate oscillations [22-24].”

At this time, it is not known conclusively whether the variation of a constant signifies that it is assuredly a dynamical field, or not, or is something else entirely. In a separate paper by this author, issues specific to the Schrödinger equation in a single-particle, non-relativistic, non-field theoretic framework for a position-dependent \hbar , that is not treated as a dynamical field, were examined [25], the reference of the excerpted section. That work is relevant to the present paper for two reasons. The first reason is that the positional variation of \hbar is derived in [25] from a completely different starting point, that results in the same in functional form as one derived in this paper.”

In this paper, variations in \hbar will be treated as a scalar dynamical field, coupling fields through the derivative terms in the Lagrangian density. The second reason is that one of the results to

follow in this paper suggests that frequency may be a more fundamental parameter than energy, and the Schrödinger equation of [25] is frequency-conserving and Hermitian. Continuing the modified excerpt from [25]:

“The scope of much work with variable constants as dynamical fields has been to address unsolved problems in cosmology. Consider the Cosmon of Wetterich [26-27], using a field dependent prefactor to the derivative term in the scalar Lagrangian that decays to a constant value for large field values, acting like variable Planck mass [27]. Existing theories with varying constants as fields are the Jordan-Brans-Dicke scalar-tensor theory developed in the late 1950’s with variable G , and Bekenstein variable fine structure constant theory developed in 1982 [28-29]. The latter did not contain gravity, and was concerned with the electromagnetic sector. Albrecht, Magueijo and Moffat, examined a variable c^4 to attempt to explain the flatness and horizon problems, the cosmological constant problem, and homogeneity problem [30]. Cosmologies of varying c were examined by Barrow [31] and Moffat [32-33].

$$S_{GR} = \int \left\{ \begin{array}{l} \frac{(c_o \mathbb{C})^4}{16G_o \pi} \xi R + \\ \frac{(\hbar_o \psi)^2}{2} g^{\mu\nu} \nabla_\mu \psi \nabla_\nu \psi + \frac{(\hbar_o \psi)^2}{2} \frac{w}{\xi} g^{\mu\nu} \nabla_\mu \xi \nabla_\nu \xi + \frac{(\hbar_o \psi)^2}{2} g^{\mu\nu} \nabla_\mu \mathbb{C} \nabla_\nu \mathbb{C} \\ + \lambda \xi \psi \mathbb{C} R + L_m \{ \hbar, c, G \} \end{array} \right\} \sqrt{-g} d^4 x \quad (1)$$

$$\frac{\partial}{\partial x_o} = \frac{1}{c_o \mathbb{C}} \frac{\partial}{\partial t} \quad (2)$$

$$G = G_o / \xi \quad (3)$$

$$\hbar = \hbar_o \psi \quad (4)$$

$$c = c_o \mathbb{C} \quad (5)$$

Equations (1) to (5) show in a single form an amalgam of possible couplings including a Jordan-Brans-Dicke-like scalar-tensor theory of alternative General Relativity with variable G , an Albrecht-Magueijo-Barrow-Moffat-like field for c , a field for \hbar like that of [28-29], which is different than the form of Bekenstein’s for variable e^2 whose representative field squared divided the derivative terms. There is also the field theory of Modified Gravity (MOG) of Moffat, and the Tensor-Vector-Scalar (TeVeS) gravity of Bekenstein. There are many ways all the constants might be represented as fields, and many ways they might be coupled. Coupling fields together in this way is the accepted approach for the treatment of a constant.”

The scalar field setup used for \hbar will couple through the derivative terms, and to itself. Cosmological and astrophysical interpretations of this setup will be developed. The fields in the prefactors to follow are literally assigned to represent Planck’s constant, distinct from c , or the fine structure constant, and e is not present.

Consider these six specifics concerning the mathematics of scalar fields:

- i. k -Essence Theory

These models were introduced as an alternative to constant dark energy, to explain the accelerated expansion of the universe, and the time evolution of the cosmological constant [37-41]. The actions involve $\mathcal{L}_k = F$ for any function the kinetic terms X and scalar field ψ , usually minimally coupled to gravity,

$$\mathcal{L}_k = F(\psi, X) \quad (6)$$

$$X = \frac{1}{2} g^{\mu\nu} \nabla_\mu \psi \nabla_\nu \psi \quad (7)$$

Thus, the k -Essence models may encompass the field to be studied here that is linear in X , and there may already be a well-studied mathematical solution that has simply not been called out as \hbar , or any other familiar constant, other than the cosmological constant.

ii. Field Redefinition

It is possible to redefine a coupled scalar field so that the kinetic terms look like that of a normal free-field theory. This is most easily accomplished when the coupling of ψ is not to the kinetic terms of another field (and in some cases when it is), and when \mathcal{L}_k is linear in X . When ψ is redefined, new interaction terms then appear in the Lagrangian, and a Hamiltonian may be derived from the Euler-Lagrange equations with respect to the new field. The perturbative expansion of QFT may then be used for the theory, and the S -matrix is not altered by the redefinition. Thus, amplitudes for various processes may be computed, despite the complexity of the original Lagrangian, with alterations in the interpretations of interaction terms and pre-factors.

iii. Canonical Quantization

The standard prescription will be applied to the most basic Klein-Gordon free-field. A variation is offered, pertaining to an infinite number of field redefinitions that the particular setup under study is amenable to.

iv. Non-Propagating Modes and Static Modes

Non-propagating modes, and also static fields, are a reasonable candidate to represent a fundamental constant, as they do not require the propagation of particles to have a remote effect. The non-propagating modes do require particles when the field values change.

v. Vacuum Solutions

The classical vacuum solutions are well known, and here are linked to non-propagating modes. Vacuum solutions were examined by the author, in which Planck's constant appears as an unnamed field in the denominator of a Lagrangian density, the field called φ in Equations (44) and (45) of [34]. The idea for that

particular Lagrangian came from a derivation using a path integral in two unpublished papers, that may presently be found in [35-36], where Planck's constant is directly identified.

vi. Tadpoles and Lagrangians with Linear Field Dependences

The coupling setup will produce a linear field interaction term (tadpole) from the mass term, inducing a non-zero vacuum expectation value (VEV). The standard treatment is to eliminate the tadpole with a field redefinition, so that the S -matrix elements can be more simply computed by normal means. Retaining the linear term, however, spoils the interpretations of mass and propagation. Here, a divergent, static classical solution will prompt the mass to be set to zero, for four reasons: the boundary condition assumed is that the field should not diverge far from the origin; the consensus is that any varying constant would be described by a nearly massless scalar field; the mathematics is simpler; terms and coefficients retain their interpretations. The tadpole may have other consequences for Planck's constant and coupling, but that will be relegated to further work.

There are a great number of rather exotic fields under study. Some have been intentionally linked to varying constants at the outset, per those in the introduction. Of those fields that have *not* already been linked to the variation of a familiar constant from the start, one may wonder if some theories might be, after the fact. Identifying them would be no small undertaking.

One objective of this effort is to publicize that mathematical solutions may already exist for fields that could represent fundamental constants, but have not been brought to light, either because of the reticence to talk about the variation of a constant, or the field was not recognized as possibly representing a constant. There is also a tendency in field theory to work in natural units, $c = G = \hbar = 1$, and this would tend to suppress thinking about new fields as representing, and evolving into, the fundamental constants with which we are most familiar. In cosmological theories, a field capable of explaining many observations, left unrecognized as a constant, inadvertently or intentionally, reduces the possibility of experimentally substantiating the theory, as it reduces the scope of experiments that might be capable of detecting its implications.

Per Occam's Razor, it is reasonable to start with theories that involve varying fields that are intentionally representative of the fundamental constants most familiar to us, reduced to the utmost of simplicity. The one that has been given minimal treatment is \hbar , now treated below, in the simplest possible case.

The paper outline is as follows: 1) The Lagrangians of importance will be developed; 2) Propagating and non-propagating mode solutions will be examined, and where possible, quantized; 3) Cosmological and astrophysical interpretations will be offered.

2. Classical Field Lagrangian Densities

Consider two symmetrically coupled scalar fields of mass m and M with coupling constant g , showing the unburied location of the constants \hbar and c in the Lagrangian density \mathcal{L} ,

$$\mathcal{L} = \frac{1}{2} \hbar^2 \partial_u \varphi \partial^u \varphi - \frac{1}{2} m^2 c^2 \varphi^2 + \frac{1}{2} \hbar^2 \partial_u \psi \partial^u \psi - \frac{1}{2} M^2 c^2 \psi^2 - g \psi \varphi \quad (8)$$

The Lagrangian density of Equation (8) produces the normal coupled Klein-Gordon equations for the fields (or particles) ψ and φ . The constant \hbar might be associated with the fields directly (though this does not matter if \hbar is just a normal constant). If so, as a prelude to making \hbar a field, it is shown as operated on by the derivatives,

$$\mathcal{L} = \frac{1}{2} \partial_u \hbar \varphi \partial^u \hbar \varphi - \frac{1}{2} m^2 c^2 \varphi^2 + \frac{1}{2} \partial_u \hbar \psi \partial^u \hbar \psi - \frac{1}{2} M^2 c^2 \psi^2 - g \psi \varphi \quad (9)$$

Whether the latter is necessary or not is an unknown, but is an option to investigate, and there are many possible coupling schemes, other than the one to be discussed.

Let it now be supposed that \hbar is itself a dynamical field, which would be a natural way to introduce it as a non-constant. If \hbar is to have the usual units of J's, the unit keeping then necessitates the introduction of yet another constant β , where $\hbar = \beta \psi$.

Selection of a Lagrangian is per Occam's Razor, and is the simplest form that combines \hbar as its own pre-factor, and as the pre-factor of all other to-be-quantized fields. From (8),

$$\mathcal{L} = \frac{1}{2} (\beta \psi)^2 \partial_u \varphi \partial^u \varphi - \frac{1}{2} m^2 c^2 \varphi^2 + \frac{1}{2} (\beta \psi)^2 \partial_u \psi \partial^u \psi - \frac{1}{2} M^2 c^2 \psi^2 - g \psi \varphi \quad (10)$$

The key idea here is that the quantum mechanical field for \hbar also functions as its own \hbar . To coin a term, the field for \hbar is its own "actionizer", and acts on all other to-be-quantized fields with the same proportionality constant β . The fields for \hbar are dubbed the "acton".

3.0 Planck's Constant as a Self-Actionizing Field in Isolation

Consider first a much more standard form of coupling. Take Equation (8) with $M=m=0$, describing two massless fields interacting through a coupling term that is separate from the derivative term. Then let the two fields be the same field, that is, let $\varphi = \psi$. Equation (8) then becomes, with \hbar a bona fide constant,

$$\mathcal{L} = \mathcal{L}_k = F(\psi, X) = \hbar^2 \partial_u \psi \partial^u \psi - g \psi^2 \quad (11)$$

The resulting equation of motion is,

$$\partial_t^2 \psi - c^2 \nabla^2 \psi + \frac{g c^4}{\hbar^2} \psi = 0 \quad (12)$$

From Equation (11) and (12) it is seen that a fields ability to couple to itself separately from the derivative term, that is it self-interacts, produces the equivalent of a mass equal to $m^2 = g$.

Quadratic self-interaction terms are interpreted as mass in a free field. In Lagrangians with additional interaction terms, there must be no linear terms if the quadratic terms are to be interpreted as a physical mass, even though the theory can still be solved. Such terms are important in symmetry breaking, but here are eliminated.

3.1 The Field Redefinition $\chi = \psi^2$

Now promote \hbar to a field $\beta\psi$, and redefine the field. An interpretation of the results will be given Section 4.0, relating results to follow to the cosmological constant.

The Lagrangian densities, equations of motion, and Hamiltonian for ψ and its redefinition $\chi = \psi^2$ are,

$$\mathcal{L}_\psi = \frac{1}{2}(\beta\psi)^2 \partial_u \psi \partial^u \psi - \frac{1}{2} M^2 c^2 \psi^2 \quad (13)$$

$$\ddot{\psi} - \nabla^2 \psi + \frac{M^2 c^2}{\beta\psi} + \frac{\dot{\psi}^2}{\psi} = 0 \quad (14)$$

$$\mathcal{H}_\psi = \frac{1}{2}(\beta\psi)^2 \dot{\psi}^2 + \frac{1}{2}(\beta\psi)^2 (\nabla\psi)^2 + \frac{1}{2} M^2 c^2 \psi^2 \quad (15)$$

$$\mathcal{L}_\chi = \frac{1}{8} \beta^2 \partial_u \chi \partial^u \chi - \frac{1}{2} M^2 c^2 \chi \quad (16)$$

$$\ddot{\chi} - \nabla^2 \chi + 4 \frac{M^2 c^2}{\beta^2} = 0 \quad (17)$$

$$\mathcal{H}_\chi = \underbrace{\frac{1}{8} \beta^2 \dot{\chi}^2 + \frac{1}{8} \beta^2 (\nabla\chi)^2}_{\mathcal{H}_\chi^f} + \underbrace{\frac{1}{2} M^2 c^2 \chi}_{\mathcal{H}_\chi^i} \quad (18)$$

Note that the mass terms of \mathcal{L}_χ and \mathcal{H}_χ , (16)x and (18) linear in χ , the tadpole. The terms no longer physically represent a mass, rather an induced non-zero vacuum expectation value (VEV). If one wishes to use χ to compute S-matrix elements, the vacuum expectation value must vanish, either by setting $M=0$, or by redefining the field again, per $\chi \rightarrow \chi - \chi^{(\text{VEV})}$. If the latter redefinition were utilized in a coupling involving more fields than χ , then all the coefficients and interaction terms in the Lagrangian would also be changed from their original interpretations.

Even more concretely, χ is not in the mass term of the equation of motion. As a result, the static *classical* solution of the equation of motion for χ diverges as r^2 . The non-propagating modes are,

here, more heavily weighted candidates to represent the familiar constants. Concerning the boundary conditions for fields that may represent physical constants, it is sensible that they should not diverge with increasing range.

For all of the reasons mentioned here and in the prior sections, Occam's Razor leads to the additional simplification that $M=0$, and the massless Klein-Gordon equation if $\chi \rightarrow 2\chi$ (although the latter will not be employed). $\hbar^2 = \beta^2\chi$ is a viable solution, provided the mass is zero, to avoid a classical solution that diverges with increasing range.

Note that the massless Klein-Gordon equation (17) with $M=0$ for the squared field $\hbar^2 = \beta^2\chi$ is equivalent to (14) with $M = 0$ for the unsquared field $\hbar = \beta\psi$. That is, the equation of motion for Planck's constant $\hbar = \beta\psi$ is not simply a massless Klein-Gordon equation for ψ , because the field must support itself. These are important results, arrived at because the field was specifically called out as representing \hbar at the beginning. Were M not zero, one of the cosmological interpretations of this field, discussed in Section 3.5, would not be possible, and the averaging scheme in Appendix 2, pertaining to the non-propagating mode solution of Section 3.3, would not produce a sensible result.

Quantization of χ follows by the standard procedure, with Fourier expansion of the fields, making Fourier coefficients operators,

$$E_\chi = \frac{1}{4} \beta^2 \int \frac{d^3 p}{(2\pi)^3} \frac{\omega_{\vec{p}}}{c} \left(a_{\vec{p}}^\dagger a_{\vec{p}} + \frac{(2\pi)^3}{2} \delta^{(3)}(0) \right) \quad (19)$$

The vacuum term has been left intentionally in (19), and the divergent term is usually explained by two singularities that arise in the treatment, the infrared and ultraviolet divergences.

It is now natural to ask whether β , the new constant, should also be represented by a field. What is interesting about this setup, is that it is amenable to repeated application of the redefinition procedure. One finds for the n^{th} repeated application,

$$\mathcal{L}_\psi^{(n)} = \frac{1}{2} \frac{1}{4^n} (\beta^{(n)})^2 \partial_u \psi^{(n+1)} \partial^u \psi^{(n+1)} \quad (20)$$

$$\beta^{(n-1)} = \beta^{(n)} \psi^{(n)} \quad (21)$$

$$\psi^{(n)} = (\psi^{(n-1)})^2 = (\psi^{(1)})^{2^n} \quad (22)$$

$$\hbar = \beta^{(n)} \prod_{i=1}^n \psi^{(i)} \quad (23)$$

$$E_\chi^{(n+1)} = \frac{1}{4^n} (\beta^{(n)})^2 \int \frac{d^3 p}{(2\pi)^3} \frac{\omega_{\vec{p}}^{(n+1)}}{c} \left(a_{\vec{p}}^{(n+1)\dagger} a_{\vec{p}}^{(n+1)} + \left(\frac{(2\pi)^3}{2} \delta^{(3)}(0) \right)^{(n+1)} \right) \quad (24)$$

Normal ordering would normally remove the vacuum term, and it would be given no further thought, though normal ordering is the equivalent of a simple subtraction of it - or of throwing it out. Intentionally leaving it, for $n=\infty$, for a finite number of particles, the term of (24) that has a clearer prospect of remaining non-zero is the vacuum term, written in (25). Without a formal investigation of the infinities, one may tentatively conclude that the energy that sustains Planck's constant is that of the vacuum,

$$E^{(\infty)} = \frac{1}{4^\infty} (\beta^{(\infty)})^2 \int \frac{d^3 p}{(2\pi)^3} \frac{\omega_{\vec{p}}^{(\infty)}}{c} \left(\frac{(2\pi)^3}{2} \delta^{(3)}(0) \right)^{(\infty)} = E^{(1)} \quad (25)$$

Further, the redefined field should have the same energy as before redefinition. Per (25), this would be possible if there are no permitted excitations of the field, that is, no particles at all, and all of the operators are zero, namely, static, and non-propagating fields.

While the argument is not rigorous, it does hint at the importance of the non-propagating modes, vacuum solutions, solutions with zero momentum, static solutions, and why such excitations are not in the common realm of experience. Despite that this manipulation may seem to be an overcomplication of the simplest solution available, this possible property of the setup is memorialized here for a simple reason: what constants actually are is not understood, and this result is an unturned stone, mathematically.

In (25), the only variable in the integrand is the frequency. In this light, one may speculate whether the most fundamental physical parameter describing the vacuum is the frequency. This was the result mentioned in the introduction that prompted the investigations made of a frequency-conserving form of the Schrödinger equation in [25].

The discussion will continue with only the first field redefinition.

3.2 Propagating and Non-Propagating Classical and Quantized Solutions for χ

Perhaps the reason there is no propagation required for a constant to have an effect is because the field associated with it has zero momentum, that is, the occupation number of the particles is zero, and the modes are non-propagating, leaving only the vacuum. From the equation of motion for χ with $M=0$, one finds by separation of variables, and completely standard canonical quantization,

$$\chi = S_\chi(\vec{r}) \varphi_\chi(x_o) \quad (26)$$

$$\frac{\ddot{\varphi}_\chi}{\varphi_\chi} = \frac{\nabla^2 S_\chi}{S_\chi} = -\frac{\omega_{\vec{p}}^2}{c^2} = -\vec{p} \cdot \vec{p} = -p^2 \quad (27)$$

$$\varphi_{\vec{p}\chi} = A_{\vec{p}} e^{i\frac{\omega_{\vec{p}}}{c} x_o} + B_{\vec{p}} e^{-i\frac{\omega_{\vec{p}}}{c} x_o} \quad (28)$$

$$S_{\vec{p}\chi} = C_{\vec{p}} e^{i\vec{p} \cdot \vec{r}} + D_{\vec{p}} e^{-i\vec{p} \cdot \vec{r}} \quad (29)$$

$$D_{\bar{p}} = A_{\bar{p}} = 0 \quad (30)$$

$$\chi_{\bar{p}} = C_{\bar{p}} B_{\bar{p}} e^{\bar{p} \cdot \bar{r} - i \frac{\omega_{\bar{p}}}{c} x_o} + c.c. = \tilde{a}_{\bar{p}} e^{\bar{p} \cdot \bar{r} - i \frac{\omega_{\bar{p}}}{c} x_o} + \tilde{a}_{\bar{p}}^* e^{-\bar{p} \cdot \bar{r} + i \frac{\omega_{\bar{p}}}{c} x_o} \quad (31)$$

$$\chi = \int \frac{d^3 p}{(2\pi)^3} \sqrt{\frac{c}{8\omega_{\bar{p}}}} \left(a_{\bar{p}} e^{i\bar{p} \cdot \bar{r}} + a_{\bar{p}}^\dagger e^{-i\bar{p} \cdot \bar{r}} \right) \quad (32)$$

$$\lim_{\bar{p} \rightarrow 0} \chi_{\bar{p}} = \chi_o = (\tilde{a}_o + \tilde{a}_o^*) \quad (33)$$

The equation of motion for χ is linear and homogeneous, allowing the sum over the solutions χ_p . In taking the limit $p \rightarrow 0$ *after* finding the solutions, it is seen that the zeroth component χ_o is constant, so $\hbar^2 = \beta^2 \chi_o$ is constant and real. Equations (26) and (27) are examined in the Appendix 1 for another solution, different than (31), and pertinent to quantization of a standing wave field.

3.3 Non-Propagating Classical Solutions for χ and ψ

Consider taking the limit $p \rightarrow 0$ *before* solving the differential equation as a vacuum (non-propagating) solution. One finds a different solution. Mathematically, it is known the limit of the solution will not equal the solution of the limit, yet, there is no reason physically to exclude either as a solution in the interest of finding new explanations for variations of constants, which are not yet well-understood. Such spatial solutions are those of Laplace's equation, the same as the equation of the Newtonian gravitational potential in vacuum, or the electric potential in vacuum. The solutions for the zero-momentum field representing \hbar^2 are therefore the allowed classical vacuum solutions. From (27) with first taking $p \rightarrow 0$,

$$\underline{S}_{o\chi}(\bar{r}) = \sum_{l=0}^{\infty} \sum_{m=0}^{\infty} \underline{S}_{o\chi}(\bar{r}) \Big|_l^m = \sum_{l=0}^{\infty} \sum_{m=0}^{\infty} (A_l r^l + B_l r^{-l-1}) P_l^m(\cos \phi) (S_m \sin(m\theta) + C_m \cos(m\theta)) \quad (34)$$

$$\underline{\varphi}_{o\chi}(x_o) = b_1 + b_2 x_o \quad (35)$$

where the underline means the limit $p \rightarrow 0$ is taken before solving the differential equation, and with the spatial form selected so as to be real. The sub- and superscripts are the azimuthal and polar indices of the solution. Of particular interest is the solution for $l=m=0$ with all other coefficients zero,

$$\underline{S}_{o\chi}(\bar{r}) \Big|_l^m = b_3 + \frac{b_4}{r} \quad (36)$$

Note that in (35) and (36) there are constants $b_{1,2,3,4}$. The first and second pertain to the time dependence (35), and the third and fourth pertain to the spatial dependence of the $l=m=0$ solution of (34), renamed for neatness.

The reason for the interest is that (36) may be always positive, real, and decays to a constant at $r=\infty$. This way, very far from the origin of the acton, which is to represent a physical constant, there is no asymmetry of behavior in space. The solutions (34) to (35) cannot be quantized. There is, however, now a classical energy associated with the solution (35) and (36), despite that momentum is zero. The Hamiltonian density is from (18), (35) and (36),

$$\underline{H}_{ox} |^0 = \frac{\beta^2}{8} \left(\left(b_2 b_3 + \frac{b_2 b_4}{r} \right)^2 + \frac{(b_1 b_4 + b_2 b_4 x_o)^2}{r^4} \right) \quad (37)$$

and Planck's constant becomes,

$$\underline{h}_{ox} |^0 = \beta \sqrt{(b_1 + b_2 x_o) \left(b_3 + \frac{b_4}{r} \right)} \quad (38)$$

It can be seen from (37) and (38) that Planck's constant, per this model, can change as a function of time and position, and, that there is an energy density associated with its existence that also changes as a function of time and position. From (34) there are many other profiles that might be explored.

Consider now another related solution path, where the field is not representative of \hbar^2 , but of \hbar . The equation of motion for ψ is now derived from Equation (13), and not its square χ . The non-linear homogeneous equation of motion is (14).

Equation (14) is separable (x_o dependent) if and only if $M=0$, another cause for this choice. Writing $\psi = S_\psi(r) \varphi_\psi(x_o)$, the equation of motion becomes, for a specific wavenumber p or frequency ω_p ,

$$\frac{\ddot{\varphi}_\psi}{\varphi_\psi} + \frac{\dot{\varphi}_\psi^2}{\varphi_\psi^2} = \frac{\nabla^2 S_\psi}{S_\psi} + \frac{(\nabla S_\psi)^2}{S_\psi^2} = -\frac{\omega_p^2}{c^2} = -p^2 \quad (39)$$

The limit $p \rightarrow 0$ is again taken first, now stipulating a radial dependence only, so using the radial term of the spherical Laplacian,

$$\underline{S}_{o\psi}(r) = \left(b_3 + \frac{b_4}{r} \right)^{1/2} \quad (40)$$

$$\underline{\varphi}_{o\psi}(x_o) = (b_1 + b_2 x_o)^{1/2} \quad (41)$$

Squaring (40) and (41), then comparing to (34) and (35), one sees they are identical. Enforcing a radial dependence in $\underline{\psi}$ produces the same solution as $l=m=0$ for $\chi=\psi^2$. One finds,

$$\underline{\psi}_o = \sqrt{\underline{\chi}_o |^0} \quad (42)$$

$$\underline{\hbar}_{o\psi} = \underline{\hbar}_{o\chi} \Big|_0^0 \quad (43)$$

$$\underline{H}_{o\psi} = \underline{H}_{o\chi} \Big|_0^0 \quad (44)$$

which is a reassuring check, showing that both representative fields are equivalent in this case. The Hamiltonian density used for (44) was (18) with $M=0$.

3.4 Another Non-Propagating Solution for χ and ψ – Standing Waves

The following is in keeping with finding solutions that far from the action origin do not show a spatial asymmetry. This is accomplished from (21) by stipulating that the solutions ψ have spherical symmetry with only a radial momentum p_r , so ψ has no angular dependence. The step produces localized standing wave solutions that do not decay in time. There are no resulting dot products of p with position r in the solutions, only the scalar product $p_r r$.

Continuing, the solutions to the non-linear equation of motion ψ_p will then be individually squared to produce ψ_p^2 , analogous to χ_p which one recalls is derived from a linear and homogeneous equation of motion, allowing solution summation. The ψ_p^2 will then be summed to form ψ^2 , followed by quantization of ψ^2 , not ψ . Proceeding in that order produces a different solution than those of Sections 3.1, 3.2, and 3.3. The Appendix 1 shows there is a more general solution, solving (26) and (27) for χ_p , and by choice of coefficients that eliminate terms, $\chi_p = \psi_p^2$, equivalent to the square of (45), (46), and to (47).

Returning to Equation (39) for $p=p_r \neq 0$, again, where there is only a radial momentum dependence, one finds,

$$S_{p\psi}(r) = d_2 \left(\frac{\cos(\sqrt{2}pr + d_1)}{\sqrt{2}pr} \right)^{1/2} \quad (45)$$

$$\varphi_{p\psi}(x_o) = d_4 \left(\cos(\sqrt{2}p(d_3 + x_o)) \right)^{1/2} \quad (46)$$

where the subscript r on p_r has been dropped. Note in that the limit of the solutions (45) and (46) does not equal the solution of the limit (40) and (41).

The factor pr is simply a scalar product, not a dot product between vectors. When squared, the solutions (45) and (46) are that of a localized spherical standing wave, not a traveling wave. This field on its own would not seem to represent a constant like \hbar very well, since (45) can be either imaginary, or when squared, negative, and in either case, falling to zero at $r=\infty$. However, the solution of (45) and (46) is of interest, because it is unusual, and also quantizable.

The profile of the field $\underline{S}_{o\psi}$ from (40) is shown in Figure 1a for various values of the constants, and the profile of $\underline{S}_{p\psi^2}$ from (45) is shown in Figure 1b.

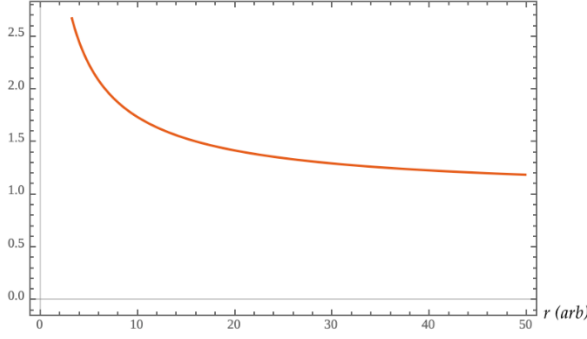


Figure 1a. $\underline{S}_{0\psi}$ field profile.

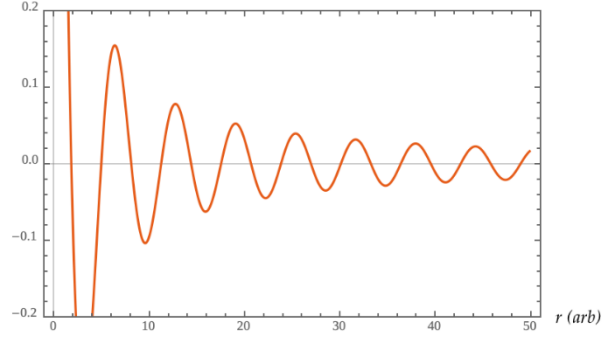


Figure 1b. $\underline{S}_{p\psi^2}$ field profile.

3.5 Canonical Quantization of the Standing Wave ψ^2 Solution

What may the $p=p_r \neq 0$ solutions, Equations (45-46), correspond to in a quantum field theory? The endeavor will be to attempt their canonical quantization, following the unusual steps outlined in the last section. Observe that the standing wave field $\underline{\psi}_p = \underline{S}_{p\psi} \underline{\varrho}_{p\psi}$ is complex, but $\underline{\psi}_p^2$ is real, spatially oscillating and decaying with an envelope $1/r$, and also oscillating with an overall amplitude in time,

$$\psi_p^2 = (d_2 d_4)^2 \left(\frac{\cos(\sqrt{2}pr + d_1)}{\sqrt{2}pr} \right) \left(\cos(\sqrt{2}p(d_3 + x_o)) \right) \quad (47)$$

Expressing (47) in exponential form, and setting d_1 and d_3 to zero,

$$\psi_p^2 = \left(\frac{1}{2} \right)^2 (d_2 d_4)^2 \frac{1}{\sqrt{2}pr} \left(e^{i\sqrt{2}pr} + e^{-i\sqrt{2}pr} \right) \left(e^{-i\sqrt{2}px_o} + e^{i\sqrt{2}px_o} \right) \quad (48)$$

In order to make the transition from (48) to an expansion, the expansion coefficients will be associated only with the time (x_o) components, and formulated so as to obey a reality condition,

$$\psi_p^2 = \left(\frac{1}{2} \right)^2 (d_2 d_4)^2 \frac{1}{\sqrt{2}pr} \left(e^{i\sqrt{2}pr} + e^{-i\sqrt{2}pr} \right) \left(\tilde{a}_p e^{-i\sqrt{2}px_o} + \tilde{a}_p^* e^{i\sqrt{2}px_o} \right) \quad (49)$$

An integration over wavenumber is performed to form the complete solution as a superposition. Note that the wavenumber integral is one dimensional, since the momentum is only radial.

$$\psi^2 = \left(\frac{1}{2} \right)^2 (d_2 d_4)^2 \int \frac{dp}{(2\pi)} \frac{1}{\sqrt{2}pr} \underbrace{\left(e^{i\sqrt{2}pr} + e^{-i\sqrt{2}pr} \right)}_{2 \cos(\sqrt{2}pr)} \left(\tilde{a}_p e^{-i\sqrt{2}px_o} + \tilde{a}_p^* e^{i\sqrt{2}px_o} \right) \quad (50)$$

As for the derivatives,

$$\partial_{x_o} \psi^2 = \left(\frac{1}{2}\right)^2 (d_2 d_4)^2 \int \frac{dp}{(2\pi)} (-i) \frac{\sqrt{\omega_p / c}}{r} \underbrace{\left(e^{i\sqrt{2}pr} + e^{-i\sqrt{2}pr}\right)}_{2\cos(\sqrt{2}pr)} \left(\tilde{a}_p e^{-i\sqrt{2}px_o} - \tilde{a}_p^* e^{i\sqrt{2}px_o}\right) \quad (51)$$

$$\nabla \psi^2 = \left(\frac{1}{2}\right)^2 (d_2 d_4)^2 \int \frac{dp}{(2\pi)} (i) \frac{\sqrt{\omega_p / c}}{r} \underbrace{\left(e^{i\sqrt{2}pr} - e^{-i\sqrt{2}pr}\right)}_{2i\sin(\sqrt{2}pr)} \left(\tilde{a}_p e^{-i\sqrt{2}px_o} + \tilde{a}_p^* e^{i\sqrt{2}px_o}\right) \quad (52)$$

Collecting factors carefully, and on quantizing, the fields become,

$$\psi^2 = \left(\frac{1}{2}\right) (d_2 d_4)^2 \int \frac{dp}{(2\pi)} \frac{1}{\sqrt{2 \cdot 8\omega_p / cr}} (a_p + a_p^\dagger) \cos(\sqrt{2}pr) \quad (53)$$

$$\partial_{x_o} \psi^2 = \left(\frac{1}{2}\right) (d_2 d_4)^2 \int \frac{dp}{(2\pi)} (-i) \frac{\sqrt{\omega_p / 8c}}{r} (a_p - a_p^\dagger) \cos(\sqrt{2}pr) \quad (54)$$

$$\nabla \psi^2 = \left(\frac{1}{2}\right) (d_2 d_4)^2 \int \frac{dp}{(2\pi)} (-1) \frac{\sqrt{\omega_p / 8c}}{r} (a_p + a_p^\dagger) \sin(\sqrt{2}pr) \quad (55)$$

The Hamiltonian density is,

$$\mathcal{H} = \frac{1}{8} \beta^2 \left(\partial_{x_o} \psi^2\right)^2 + \frac{1}{8} \beta_{\psi\psi}^2 \left(\nabla \psi^2\right)^2 \quad (56)$$

and the total energy,

$$E = \frac{1}{8^2} \beta^2 (d_2 d_4)^4 \left(\frac{1}{2}\right)^2 \int d^3r \frac{dpdk}{(2\pi)^2} \frac{\sqrt{\omega_p \omega_k}}{cr^2} \times \left(\begin{aligned} &(-1) \cos(\sqrt{2}pr) \cos(\sqrt{2}kr) (a_p - a_p^\dagger) (a_k - a_k^\dagger) \\ &+ \\ &(+1) \sin(\sqrt{2}pr) \sin(\sqrt{2}kr) (a_p + a_p^\dagger) (a_k + a_k^\dagger) \end{aligned} \right) \quad (57)$$

Multiplying out (57), rearranging terms, integrating over spatial angles, and cancelling the r^2 from the denominator stemming from the spatial integral,

$$E = \frac{\pi}{8^2} \beta^2 (d_2 d_4)^4 \int \frac{dp dk}{(2\pi)^2} \frac{\sqrt{\omega_p \omega_k}}{c} \times \left(\begin{aligned} & \left(a_p a_k^\dagger + a_p^\dagger a_k \right) \int dr \underbrace{\left(\sin(\sqrt{2}pr) \sin(\sqrt{2}kr) + \cos(\sqrt{2}pr) \cos(\sqrt{2}kr) \right)}_{(2\pi)\delta(k-p)} \\ & + \\ & \left(a_p a_k + a_p^\dagger a_k^\dagger \right) \int dr \underbrace{\left(\sin(\sqrt{2}pr) \sin(\sqrt{2}kr) - \cos(\sqrt{2}pr) \cos(\sqrt{2}kr) \right)}_{-(2\pi)\delta(k+p)} \end{aligned} \right) \quad (58)$$

The interpretation of the formally non-convergent integral is shown in the under-brackets of (58). Continuing,

$$E = \frac{\pi}{8^2} \beta^2 (d_2 d_4)^4 \int \frac{dp}{(2\pi)} \frac{\omega_p}{c} \left(\left(a_p a_p^\dagger + a_p^\dagger a_p \right) - \underbrace{\left(a_p a_{-p} + a_p^\dagger a_{-p}^\dagger \right)}_0 \right) \quad (59)$$

$$E = \frac{\pi}{32} \beta^2 (d_2 d_4)^4 \int \frac{dp}{(2\pi)} \frac{\omega_p}{c} \left(a_p^\dagger a_p + \underbrace{\frac{(2\pi)}{2} \delta^{(1)}(0)}_\infty \right) \quad (60)$$

$$:E := \frac{\pi}{32} \beta^2 (d_2 d_4)^4 \int \frac{dp}{(2\pi)} \frac{\omega_p}{c} a_p^\dagger a_p \quad (61)$$

Well-defined quantization immediately follows if the integrals are restricted to range from $p=0$ to $p=+\infty$, where equivalently the creation and annihilation operators for states with subscripts that are negative are taken to be zero in (59), so (60) results. One may simply take this as a condition necessary to achieve quantization with no further explanation. However, a physical rationale will be offered.

Standing waves are formed from oppositely directed traveling waves. The classical solution (47) does not rely on the $-p$ solutions to combine with the $+p$ solutions to form the standing wave – it is a steady state spherical standing wave in and of itself already, describing the situation long after transient behavior is over, after setup. Now visualize the early transient behavior whereby the standing wave comes about. The acton emits a traveling spherical wave from its origin that propagates outward into space, and to develop the spherical standing wave (47), this emitted wave would have to somehow reflect off of a perfectly symmetrical spherical boundary and be directed back to the origin to interfere with the emitted wave. However, there is no physical boundary to provide reflection, so how can this occur? Assume closed curvature in the Universe during the initial field set-up, before Inflation drives the Universe to the critical density, and flat spacetime. Impose periodic boundary conditions with allowed wavevectors incremented by $2\pi/L$, where L is the period of the boundary taken to the limit $L=\infty$. Each point on the traveling spherical wavefront emitted from the origin at $r=0$ travels full circle, returning from $r=\infty$ to the

origin from the *opposite* side it was emitted from, and then interferes with the emitted wave. So, for the $+p$ states, which are initially outgoing waves emitted from the origin,

$$\underbrace{\frac{e^{+i\sqrt{2}|p|r-i\sqrt{2}\omega_p t}}{2^{3/2}|p|r}}_{\text{emitted, } r=0} + \underbrace{\frac{e^{-i\sqrt{2}|p|r-i\sqrt{2}\omega_p t}}{2^{3/2}|p|r}}_{\text{returning, } r=\infty} \propto \frac{\cos(\sqrt{2}|p|r)}{\sqrt{2}|p|r} \cos(\sqrt{2}\omega_p t) \quad (62)$$

and (39) is becomes the standing spherical wave (47) for $+p$ after taking the real part. The $-p$ states must then be initially inbound waves emitted from a spherical boundary at $r=\infty$ traveling to the origin at $r=0$, and forming the standing wave with the wave also traveling inbound from infinity that passed through the origin from the opposite side,

$$\underbrace{\frac{e^{-i\sqrt{2}|p|r-i\sqrt{2}\omega_p t}}{-2^{3/2}|p|r}}_{\text{emitted, } r=\infty} + \underbrace{\frac{e^{i\sqrt{2}|p|r-i\sqrt{2}\omega_p t}}{-2^{3/2}|p|r}}_{\text{passthrough, } r=0} \propto \frac{\cos(\sqrt{2}|p|r)}{-\sqrt{2}|p|r} \cos(\sqrt{2}\omega_p t) \quad (63)$$

So, it can be seen that the real part of (63) is the solution (47) for $-p$. However, the case of a distant boundary of sources miraculously located for simultaneous convergence on the acton center feels as unphysical as a distant reflective boundary, even though mathematically the solution is allowed, and the steady state behavior differs by only a phase of π between $+p$ and $-p$.

If there had in the distant past been closed curvature in the Universe, in the equilibration period after the Big Bang, but before Inflation at 10^{-36} s, the acton field could have been set up, interfered with itself, and then expanded during Inflation.

What is the acton origin? The following is postulated:

- i. In all the above scenarios applied to cosmology, the acton origin would be every point in the universe, if the Cosmological Principle is to be obeyed. The Planck's constant experienced on the cosmological scale would be then be a spatial average, something like the root-mean square value of (45) and (40), subject to boundary conditions that prevent its divergence, leaving a cosmological time dependence per (46) and (41). This is the background value of \hbar . A variation on this idea is treated in Appendix 2.
- ii. The infinite number of cosmological origins (every point in space) may also be thought of as coinciding with a location of *initially* infinite energy density that *does not persist*.
- iii. The field at a single origin in isolation is divergent per (47). However, the average of all origins includes an infinite number of effectively zero values, and the field can be quantized without divergence. Therefore, the averaging produces a finite value, see Appendix 2.
- iv. On astrophysical scales, in this epoch, where localized energy densities are not uniform, that *do persist*, such as supermassive black holes, neutron stars, and white

dwarfs, then (40-41) and (45-46) would represent more local perturbations those objects around the background value, so not subject to an averaging process.

Whatever the acton origin is, to quantize this field, it must be thought of as the source of the activity, the integrals dp range from $p=0$ to ∞ , the operators with negative subscripts are zero, and the second term of (59) is zero.

Then normal ordering eliminates the vacuum term in (60) giving the field quanta and their energies, (61).

The commutation relationships used were,

$$\left[a_p, a_k^\dagger \right] = (2\pi)\delta^{(1)}(p-k) \quad (64)$$

$$\left[a_p^\dagger, a_k^\dagger \right] = \left[a_p, a_k \right] = 0 \quad (65)$$

from which may be derived the relationship between conjugate variables,

$$\left[\psi^2(r), \psi^2(r') \right] = \left[\partial_{x_o} \psi^2(r), \partial_{x_o} \psi^2(r') \right] = 0 \quad (66)$$

$$\left[\psi^2(r), \partial_{x_o} \psi^2(r') \right] = i \left(\frac{(d_2 d_4)^2}{16\sqrt{2}} \right) \delta^{(1)}(r-r') \quad (67)$$

where (65) is arrived at in interpreting the following integral that results during the analysis,

$$\int dp \frac{\cos(\sqrt{2}pr) \cos(\sqrt{2}pr')}{rr'} = (2\pi)\delta^{(1)}(r-r') \quad (68)$$

The final result (61) resembles those of normal free fields, save for the pre-factors, and that the operators are left dimensioned.

4. Calibration of Coefficients

It is conjectured here that the static, non-propagating modes that couple to other fields in the derivative terms is, from (41) or (38), the square of (69). This is because it is the only solution for \hbar that is positive and real at all times. The free-field solution, and standing-wave solutions result during temporary adjustments to this non-propagating mode.

From (69) follow other relations to be used in the calibration of the coefficients,

$$\underline{\hbar}_{ov}(r,t) = \beta \sqrt{b_1 b_3 \left(1 + \frac{b_2}{b_1} x_o \right) \left(1 + \frac{b_4}{b_3} r \right)} \quad (69)$$

$$\underline{\hbar}_{ov}(\infty, t) = \beta \sqrt{b_1 b_3 \left(1 + \frac{b_2}{b_1} ct \right)} \quad (70)$$

$$\hbar_m = \underline{\hbar}_{ov}(\infty, t_H) \quad (71)$$

$$\frac{\partial_t \underline{\hbar}_{ov}(r, t)}{\underline{\hbar}_{ov}(r, t)} = \frac{1}{2} \frac{c}{(b_1 / b_2 + ct)} \Big|_{t_H} = -\frac{\partial_t \alpha}{\alpha} = 4.73 \times 10^{-18} [\text{yr}^{-1}] \quad (72)$$

The value that is measured now is \hbar_m and t_H is the Hubble time. The position dependence of $\underline{\hbar}_{ov}$ is thought provoking, see [25] and its relevant equation (97) reproduced in Section 6, and [42]. Equation (97) describes the variation of scalar fields coupled to a gravitational field when the coupling is weak [42]. Equation (98) is derived in this paper from (69), although gravity was only obliquely involved, in the curvature discussion, Section 3.5. They are very similar in appearance.

In (72), α is the fine structure constant, and the value for its time dependence comes from references [4-6]. For $t=t_H$, one then finds when attributing all the variation in the fine structure constant to Planck's constant,

$$b_1 / b_2 = 10^{33} [m] \quad (73)$$

where (73) suggests Planck's constant is slowly increasing.

From (70-71) and (73), again putting $t=t_H$, one finds,

$$\beta^2 b_2 b_3 = \frac{\hbar_m^2}{(b_1 / b_2 + ct_H)} \sim 1.11 \times 10^{-101} [\hbar^2 / m] \quad (74)$$

It was conjectured in Section 3.1 and 3.2 that the energy density associated with the constant \hbar when the field has no momentum is that of the vacuum. Now that will be followed up on.

Note the following:

- i. Arguments were given that the solution (69) for Planck's constant is associated with vacuum energy, and it is a vacuum solution.
- ii. Planck's constant is small.
- iii. The Cosmological Constant, the gravitational vacuum energy density, and the only vacuum for which an experimental value of an energy density exists, is also small.
- iv. Quantum mechanical effects are thought to be critically important at the energy scale of the pre-inflation universe, and at the singularities of black holes.
- v. Planck's constant governs all of the known quantum mechanical interactions.

- vi. The non-propagating solutions are the most simple and reasonable candidate fields to assign to the present epoch. Fundamental constants must be changing very slowly. Therefore, there are a minimal number of particles needed to readjust them at this time, so we do not commonly find them.
- vii. The electromagnetic vacuum energy density is formally divergent, and 10^{120} orders of magnitude larger than the cosmological constant when an upper bound of the Planck frequency is imposed. The vacuum catastrophe is still unresolved, and is the premier example concerning the viability of field theory, as its gravitational influence should be enormous, and it is not sensed at all. This is indicative of the lack of some fundamental understanding of fields, so is also avoided here, the standard approach in field theory.

Therefore, from (37), very far from the acton origin, the gravitational cosmological constant is equated to the energy density of the field $\hbar^2 = \beta^2 \chi$,

$$\underline{H}_{oz} \Big|_0^0 (r = \infty) = \frac{\beta^2 (b_2 b_3)^2}{8} = \Lambda = 5.63 \times 10^{-10} [J / m^3] \quad (75)$$

From (74) and (75),

$$b_2 b_3 = 3.86 \times 10^{92} [J^{-1} m^{-2} s^{-2}] \quad (76)$$

$$\beta = 1.70 \times 10^{-97} [kg^{3/2} m^{7/2} / s] \quad (77)$$

$$b_1 b_3 = 3.86 \times 10^{125} [J^{-1} m^{-1} s^{-2}] \quad (78)$$

From (44a),

$$\frac{\partial_r \underline{\hbar}_{ovr}}{\underline{\hbar}_{ovr}} = -\frac{1}{2} \frac{b_4}{b_3} \frac{1}{r^2} \frac{1}{\left(1 + \frac{b_4 / b_3}{r}\right)} \Bigg|_{R_o} \approx \frac{\delta \hbar}{\hbar} \frac{1}{\Delta R_o} = -3.5 \times 10^{-15} [m^{-1}] \quad (79)$$

$$b_4 / b_3 = 1.62 \times 10^8 [m] \quad (80)$$

The numerical value in (79) comes from the work of Hutchin [19] where it was surmised \hbar varies by 21 ppm across the Earth's orbit of radius $R_o \sim 1.52 \times 10^{11}$ m and the difference between the maximum and minimum radii $\Delta R_o = 6 \times 10^9$ m.

From (76),(78) and (80), Planck's constant is positive, and decreases with distance from the origin. In [25], single particle wavefunctions were found to be concentrated in regions of lower \hbar .

5. Coupling to Other Fields

The equations of motion for the fields coupled by the dynamical terms can only be solved analytically in the simplest of cases, but that shall be the goal here. The Lagrangian will be written in terms of the “supporting field” χ , and the “supported field” φ , so-called because χ supports the dynamical terms of φ , and also, because these fields did not get along very well, and χ had higher income.

Both fields are taken as massless, and recalling $\hbar^2 = \beta^2 \chi$. The Lagrangian is,

$$\mathcal{L} = \frac{1}{2} \beta^2 \chi \partial_u \varphi \partial^u \varphi + \frac{1}{8} \beta^2 \partial_u \chi \partial^u \chi \quad (81)$$

The equations of motion for χ and φ are, respectively,

$$\frac{1}{4} (\ddot{\chi} - \nabla^2 \chi) - \frac{1}{2} (\dot{\varphi}^2 - (\nabla \varphi)^2) = 0 \quad (82)$$

$$(\dot{\chi} \dot{\varphi} + \chi \ddot{\varphi}) - (\nabla \chi \cdot \nabla \varphi + \chi \nabla^2 \varphi) = 0 \quad (83)$$

The variable Planck’s constant field will now be shown to cause an alteration in the solution of the supported field from its free state.

The situations when the second term of (82) is zero are the easiest to solve for. Then φ is close to the form of a plane wave, φ does not influence the form of χ , and solutions for the latter already developed may be used, namely, those of (35) and (36). Therefore, the equation of motion (83) can be solved with χ as an input from its solution, in isolation, for the limit $p=0$, taken first.

The following will be needed,

$$\chi = \underline{\chi}|_0^0 \quad (84)$$

$$\underline{\chi}|_0^0 = (b_1 + b_2 x_o) \left(b_3 + \frac{b_4}{r} \right) \quad (85)$$

$$\dot{\underline{\chi}}|_0^0 = b_2 \left(b_3 + \frac{b_4}{r} \right) \quad (86)$$

$$\nabla \underline{\chi}|_0^0 = -b_4 \frac{(b_1 + b_2 x_o)}{r^2} \quad (87)$$

$$\frac{\dot{\underline{\chi}}|_0^0}{\underline{\chi}|_0^0} = \frac{b_2}{(b_1 + b_2 x_o)} \quad (88)$$

$$\frac{\nabla \chi|_0^0}{\chi|_0^0} = \frac{-b_4}{(b_3 r^2 + b_4 r)} \quad (89)$$

$$\hbar^2 = \beta^2 \chi \quad (90)$$

For $r \rightarrow \infty$, the gradient of χ is zero, and (83) becomes,

$$\frac{\dot{\chi}}{\chi} \dot{\phi} + \ddot{\phi} - \nabla^2 \phi = 0 \quad (91)$$

For very early times $x_0=0$, and from (89), (91) becomes, writing $\phi=T(t)Z(r)$ and separating variables,

$$\omega_h = \frac{b_2}{b_1} c \sim 10^{-25} [s^{-1}] \quad (92)$$

$$\omega_h \partial_t T + \partial_t^2 T = -\omega_p^2 T \quad (93)$$

$$\nabla^2 Z = -p^2 Z \quad (94)$$

$$\phi = \left(A e^{\bar{p} \cdot \bar{r}} + B e^{-\bar{p} \cdot \bar{r}} \right) \left(C e^{-\frac{t}{2}(\sqrt{\omega_h^2 - 4\omega_p^2} + \omega_h)} + D e^{\frac{t}{2}(\sqrt{\omega_h^2 - 4\omega_p^2} - \omega_h)} \right) \quad (95)$$

One sees that the supported field ϕ has been altered from the free-field solution due to the variable Planck's constant. For $\omega_h=0$, the supported field ϕ would be a pure planewave and free-field.

Based on the calibration of the constants, even at a time of $t_H \sim 10^{17}$ [s], the solution (95) is almost that of a plane wave for any reasonable value of frequency ω_p , but with a very small decay in time, controlled by ω_h , a parameter describing the temporal variation of Planck's constant.

One finds with the calibrated parameters, that the increase of \hbar with time causes the supported field amplitudes to decay in time.

The plane wave condition for the second term of (82) being approximately zero is therefore satisfied, and for $\omega_h t$ so small, it is clear how to quantize (95) for early times – simply neglect $\omega_h t$ and proceed with canonical quantization.

6. Discussion

From [25], now reproduced *verbatim*:

“Field Theory and General Relativity are the cornerstones of modern physics. There seem to be some inherent contradictions in both theories. For example, in field theory, a static field functions much like the fields as envisioned by Faraday. Yet, a static field can be approximated with the tree-level terms of the perturbative expansion to produce an amplitude, with Feynman diagrams showing particle exchange limiting the interaction to the speed of light, equated to the Born approximation amplitude to produce a classical potential. Propagation of a field would therefore appear to be required for the static field to function. For a black hole, the mass, charge, and angular momentum are not censored: they are communicated by non-propagating modes in field theory, the accepted explanation. Changes in the static fields are propagated at the speed of light, but once reestablished, are Faraday-like static fields once again, influencing instantaneously at a distance. Physical constants would be static fields, and like any static field, described by non-propagating modes, Faraday-like, influencing instantaneously at a distance. When matter or charges gravitate into the event horizon of a black hole, the initial non-propagating modes, understood to have been set up long ago, quickly readjust, to produce the new non-propagating mode. Yet, the despite the censorship of the event horizon, somehow, in the particle picture, particles (fields) must propagate from the event horizon to reset the non-propagating modes – thus emission of particles from the horizon would seem to be needed. The descriptions conflict, despite the predictive power. As to General Relativity, it is perfectly acceptable at this time, that energy and momentum are not conserved when there are dynamical changes in spacetime, although *how* the non-conservation evolves is well understood, with the conservation possible only in a locally flat frame. With a cosmological constant, the total energy of the universe increases (explained by negative pressure). The variation of physical constants throughout the universe may also constitute other acceptable violations of conservation laws.”

An object called an acton has been so named to make referring to it easier. The name encompasses:

1. the classical zero-momentum non-propagating solution
2. the classical and quantum non-propagating standing wave solution
3. the standard free-field solution

Solutions 1 and 2 are thought to be coincident with regions of high energy density, and to describe variations about the cosmological background value of \hbar , set by an averaging procedure, leaving only a cosmological temporal variation. Solution 2 could be quantized with a rationale requiring a periodic boundary conditions occurring in the early universe. They are also thought to describe local perturbations in the present epoch, about massive objects whose energy density is persistent.

Solutions for a supported scalar field were found using the zero-momentum solution of the supporting field when far from the origin of the acton. The supported field solution acquires an exponential decay beyond the free field, where the exponential decay constant is proportional to the time evolution parameter of the supporting field. The calibration suggests that Planck’s constant is increasing slowly, and that the amplitudes of supported fields decay with time. Close to the origin, the behavior is more complicated, and requires solving the differential equations numerically.

The supporting field solution resembles the position dependent Planck’s constant arrived at in reference [25] using a general relativistic argument, shown in (97), to which can be compared the result from field theory of this work (98),

$$\frac{\hbar(r)}{\hbar_\infty} = \left(1 - \beta_h \frac{R_S}{r}\right)^{1/2} \quad (97)$$

$$\frac{\hbar_{\text{acton}}(r, t)}{\hbar_{\text{acton}}(\infty, t)} = \left(1 + \frac{b_4/b_3}{r}\right)^{1/2} \quad (98)$$

In (97), β_h is the Local Position Invariance (LPI) violation parameter for Planck's constant, R_S is the Schwarzschild radius. The expressions come from completely different starting points. Comparing (97-98), one is prompted to conclude the origin of the acton coincides with the origin of a massive body. The word "coincide" was used, since the acton here is actually massless. Using the mass of the sun and (97), and the value of b_4/b_3 from the calibration in (98), one finds $\beta_h = -5.43 \times 10^4$, larger than any LPI violation ever measured. The action may coincide with mass, but b_4/b_3 is concluded not to be dependent on mass-energy, at least with the presently available information used for the calibration. The result is sensible since (98) did not involve gravity when derived.

The standing spherical wave solution is the most easily related to early quantum cosmology. It spatially decays to zero far from its origin. It could be quantized, showing energy quanta similar in form to a free field, if only positive radial momentum states are allowed. To try to rationalize this requirement, the traveling waves that comprise the standing wave were interpreted to circulate continually through an infinitude of origins (to be consistent with the cosmological principle), to infinity and back around to the other side, due to imposed periodic boundary conditions from closed curvature. The field is postulated to have been set up in the 10^{-36} s dwell time after the Big Bang, and prior to Inflation, when and if the Universe had closed curvature, before being driven flat by Inflation. Neither expansion, or closed curvature is accounted for in the equations from which the result was derived.

Whether the three fields coexist is unknown.

7. Conclusions

This a fertile area of research related to the cosmon, inflation, the inflaton, the cosmological constant, the origin of physical constants, quintessence, accelerated expansion, "dark entities", CMB anisotropy, and the possible relationships between all of them.

It would be worthwhile to determine if there are any mathematical studies of fields that have *not* yet been directly correlated to variations in the physical constants most familiar us. To find these examples, a significant undertaking in itself, would result in much shorter new papers, focusing on the interpretations and implications of the existing solutions in this light. The uncorrelated work, having not been focused on the objective of understanding constants, may be especially difficult to recognize, and the setups steered towards final solution sets that are unrecastable. The author can attest to the rarity of finding literature discussing variations of Planck's constant directly. Masters of field theory are encouraged to examine whether the more exotic fields that described the early universe also evolved into the constants of today. For any fundamental constant, direct and open theories concerning their variation would lead to a larger scope of

experiments aimed at validating predictions. Such experiments do not have to be astrophysical or cosmological, the present focus of most work on the subject at present. Older cosmological theories, newly constant-correlated, would benefit by the latter.

8. Acknowledgements

This manuscript has been released as a pre-print at arXiv, ([Dannenberg]), <https://arxiv.org/abs/1812.02325> , and is reference [43].

9. References

- [1] P. A. M. Dirac, A New Basis for Cosmology. Proc. Royal Soc. London A 165 (921) 199–208 (1938)
- [2] A. P. Meshik, The Workings of an Ancient Nuclear Reactor, Scientific American, January 26, (2009)
- [3] J.-P. Uzan and B. Leclercq, The Natural Laws of the Universe: Understanding Fundamental Constants. Springer Science & Business Media, (2010)
- [4] J. K. Webb, M. T. Murphy, V. V. Flambaum, V. A. Dzuba, J. D. Barrow, C. W. Churchill, and A. M. Wolfe, Further evidence for cosmological evolution of the fine structure constant. Phys. Rev. Lett. 87(9), 091301 (2001)
- [5] Sze-Shiang Feng, Mu-Lin Yan, Implication of Spatial and Temporal Variations of the Fine-Structure Constant, Int. J. Theor. Phys. 55, 1049–1083 (2016)
- [6] L. Kraisselburd, S. J. Landau, and C. Simeone, Variation of the fine-structure constant: an update of statistical analyses with recent data. Astronomy & Astrophysics 557, (2013)
- [7] G. Mangano, F. Lizzi, and A. Porzio, Inconstant Planck’s constant, Int. J. of Mod. Phys. A 30(34) (2015) 1550209
- [8] Maurice A. de Gosson, Mixed Quantum States with Variable Planck’s Constant, Physics Letters A Volume 381, Issue 36, Pages 3033-303 (2017)
- [9] Jean-Philippe Uzan, The fundamental constants and their variation: observational and theoretical status, Reviews of Modern Physics, 75, 403-455 (2003)
- [10] J. Kentosh and M. Mohageg, Global positioning system test of the local position invariance of Planck’s constant, Phys. Rev. Lett. 108(11) (2012) 110801
- [11] J. Kentosh and M. Mohageg, Testing the local position invariance of Planck’s constant in general relativity. Physics Essays 28(2), 286–289 (2015)

- [12] Sven Herrmann, Felix Finke, Martin Lulf, Olga Kichakova, Dirk Puetzfeld, Daniela Knickmann, Meike List, Benny Rievers, Gabriele Giorgi, Christoph Günther, Hansjörg Dittus, Roberto Prieto-Cerdeira, Florian Dilssner, Francisco Gonzalez, Erik Schönemann, Javier Ventura-Traveset, and Claus Lämmerzahl, Test of the Gravitational Redshift with Galileo Satellites in an Eccentric Orbit Phys. Rev. Lett. 121, 231102 (2018)
- [13] Ellis, K.J., The Effective Half-Life of a Broad Beam $^{238}\text{Pu}/\text{Be}$ Total Body Neutron Radiator. Physics in Medicine and Biology, 35, 1079-1088(1990)<http://dx.doi.org/10.1088/0031-9155/35/8/004>
- [14] Falkenberg, E.D., Radioactive Decay Caused by Neutrinos? Apeiron, 8, 32-45(2001)
- [15] Alburger, D.E., Harbottle, G. and Norton, E.F., Half-Life of ^{32}Si . Earth and Planetary Science Letters, 78, 168-176(1986). [http://dx.doi.org/10.1016/0012-821X\(86\)90058-0](http://dx.doi.org/10.1016/0012-821X(86)90058-0)
- [16] Jenkins, J.H., et al., Analysis of Experiments Exhibiting Time Varying Nuclear Decay Rates: Systematic Effects or New Physics?(2011) <http://arxiv.org/abs/1106.1678>
- [17] Parkhomov, A.G., Researches of Alpha and Beta Radioactivity at Long-Term Observations.(2010) <http://arxiv.org/abs/1004.1761>
- [18] Siegert, H., Schrader, H. and Schötzig, U., Half-Life Measurements of Europium Radionuclides and the Long-Term Stability of Detectors. Applied Radiation and Isotopes, 49, 1397(1998).[http://dx.doi.org/10.1016/S0969-8043\(97\)10082-3](http://dx.doi.org/10.1016/S0969-8043(97)10082-3)
- [19] Richard A. Hutchin, Experimental Evidence for Variability in Planck's Constant, Optics and Photonics Journal, 6, 124-137 (2016)
- [20] Cooper, P.S. (2008) Searching for Modifications to the Exponential Radioactive Decay Law with the Cassini Spacecraft.<http://arxiv.org/abs/0809.4248>
- [21] Norman, E.B., Browne, E., Chan, Y.D., Goldman, I.D., Larimer, R.-M., Lesko, K.T., Nelson, M., Wietfeldt, F.E. and Zlimen, I., Half-Life of ^{44}Ti . Physical Review C, 57 (1998)
- [22] E. N. Alexeyev, Ju. M. Gavriljuk, A. M. Gangapshev, A. M. Gezhaev, V. V. Kazalov, V. V. Kuzminov, S. I. Panasenko, S. S. Ratkevich, S. P. Yakimenko, Experimental test of the time stability of the half-life of alpha-decay Po-214 nuclei, (2011) <https://arxiv.org/abs/1112.4362>
- [23] Eric B. Norman, Additional experimental evidence against a solar influence on nuclear decay rates (2012) <https://arxiv.org/abs/1208.4357>
- [24] Karsten Kossert, Ole Nähle, Disproof of solar influence on the decay rates of $^{90}\text{Sr}/^{90}\text{Y}$ (2014) <https://arxiv.org/abs/1407.2493>

- [25] Rand Dannenberg, Position Dependent Planck's Constant in a Frequency-Conserving Schrödinger Equation, *Symmetry* (2020), 12, 490; doi:10.3390/sym12040490
<https://www.mdpi.com/2073-8994/12/4/490>
- [26] C. Wetterich, Naturalness of exponential cosmon potentials and the cosmological constant problem (2018), preprint <https://arxiv.org/abs/0801.3208>
- [27] C. Wetterich, Cosmon inflation. (2013) preprint <https://arxiv.org/abs/1303.4700>
- [28] J.D.Bekenstein, Fine-structure constant: Is it really a constant, *Phys. Rev. D* 25,1527 (1982).
- [29] J.D. Bekenstein, Fine-structure constant variability, equivalence principle and cosmology, *Phys. Rev. D* 66, 123514 (2002).
- [30] A. Albrecht; J. Magueijo, A time varying speed of light as a solution to cosmological puzzles. *Phys. Rev. D* 59 (4): 043516 (1999).
- [31] J.D. Barrow, Cosmologies with varying light-speed. *Physical Review D*. 59 (4): 043515 (1998)
- [32] J. W. Moffat, Superluminary universe: A Possible solution to the initial value problem in cosmology *Int.J.Mod.Phys. D* 2 351-366 (1993)
- [33] J. W. Moffat, Variable Speed of Light Cosmology, Primordial Fluctuations and Gravitational Waves, *Eur. Phys. J. C* 76:13 (2016)
- [34] Rand Dannenberg, Excluded Volume for Flat Galaxy Rotation Curves in Newtonian Gravity and General Relativity, *Symmetry* 2020, 12, 398; doi:10.3390/sym12030398,
<https://www.mdpi.com/2073-8994/12/3/398>
- [35] Rand Dannenberg, Applications of a Feynman Path Integral for Position Dependent Planck's Constant (2019), [arXiv:1812.02325](https://arxiv.org/abs/1812.02325) [quant-ph], <https://arxiv.org/abs/1812.02325>
- [36] Rand Dannenberg, Einstein-Hilbert Action And Matter Action With A Particular Scalar Field Dependence (2019), DOI: 10.13140/RG.2.2.27863.32168/20,
https://www.researchgate.net/publication/333704308_Einstein-Hilbert_Action_and_a_Matter_Action_with_a_Particular_Scalar_Field_Dependence
- [37] C.R. Almeida, J.C. Fabris, F. Sbisá, and Y. Tavakoli, Quantum cosmology with k-Essence theory, proceedings of the 31st International Colloquium on Group Theoretical Methods in Physics. Rio de Janeiro, Brazil, 19-25 June 2016 <https://arxiv.org/abs/1604.00624v2>
- [38] Alexander Vikman, K-essence: cosmology, causality and emergent geometry, Doctoral Dissertation Ludwig-Maximilians-Universität München (2007)

[39] Rubén Cordero, Eduardo L. González, Alfonso Queijeiro, An equation of state for purely kinetic k-essence inspired by cosmic topological defects, (2016)
<https://arxiv.org/abs/1608.06540v2>

[40] C. Armendáriz-Picón, T. Damour, V. Mukhanov, k -Inflation, Phys.Lett.B458:209-218, (1999), <https://arxiv.org/abs/hep-th/9904075v1>

[41] Rong-Jia Yang, Xiang-Ting Gao, Phase-space analysis of a class of k-essence cosmology, Class.Quant.Grav.28:065012,(2011) <https://arxiv.org/abs/1006.4986v3>

[42] Berengut, J.C.; Flambaum, V.V.; Ong, A.; Webb, J.K.; Barrow, J.D.; Barstow, M.A.; Holberg, J.B. Limits on the dependence of the fine-structure constant on gravitational, potential from white-dwarf spectra. Phys.Rev. Lett. (2013), 111, 010801.

[43] Rand Dannenberg, Planck's Constant As A Dynamical Field (2020), [arXiv:1812.02325](https://arxiv.org/abs/1812.02325) [quant-ph], <https://arxiv.org/abs/1812.02325>

Appendix 1

From (26) and (27), a more general alternative solution is,

$$S_{p\chi}(r) = u_1 e^{-ipr} - \frac{i u_2 e^{ipr}}{2pr} \quad (\text{A1})$$

$$\varphi_{p\chi}(x_o) = u_3 \sin(px_o) + u_4 \cos(px_o) \quad (\text{A2})$$

However, in this solution $\chi_p \neq \psi_p^2$ and there would be additional cross terms in the construction of the full χ when squaring the sum of the ψ_p .

Setting $u_1 = u_3 = 0$, $u_2 = 2i(d_2)^2$, $u_4 = (d_4)^2$, and $p \rightarrow (2)^{1/2}p$, one finds,

$$\chi_p = (d_2 d_4)^2 \frac{\exp(i\sqrt{2}pr)}{\sqrt{2}pr} \cos(\sqrt{2}px_o) \quad (\text{A3})$$

Taking the real part of (A3) results in (47) for $d_1 = d_3 = 0$, reproducing the special case when $\chi_p = \psi_p^2$, and the solutions can be summed (integrated).

An additional unstudied solution is therefore also constituted by (A1) and (A2), for which $\chi_p \neq \psi_p^2$.

Appendix 2

Consider solutions (35) and (36) for χ . To be consistent with the Cosmological Principle, the solution must be sourced at every position in space. Averaging (36) over a spherical volume V of radius R , and then taking the limit $R=\infty$, one finds,

$$\langle \hbar^2 \rangle_V = \beta^2 \langle \chi \rangle_V = \beta^2 b_1 b_3 \left(1 + \frac{b_2}{b_1} ct \right) = \underline{\hbar}_{ov}^2(\infty, t) \quad (\text{A4})$$

The latter was defined in (70), has only a temporal dependence, and is finite, despite the divergence of (35) prior to averaging.

Applications of a Feynman Path Integral for a Position Dependent Planck's Constant

Rand Dannenberg
Optical Physics Company, Simi Valley, CA 93063
e-mail: rdannenberg@opci.com

January 24, 2019

Abstract: There is controversial evidence that Planck's constant shows unexpected variations with altitude above the earth due to Kentosh and Mohageg, and yearly systematic changes with the orbit of the earth about the sun due to Hutchin. Many others have postulated that the fundamental constants of nature are not constant either locally, or universally. This work is a mathematical study, examining the impact of a position dependent Planck's constant on the Feynman path integral, using results from prior papers by the author. A derivation is shown for how the integrand in the path integral exponent becomes $L_c/\hbar(r)$, where L_c is the classical action. The path that makes stationary the integral in the exponent is termed the "dominant" path, and deviates from the classical path systematically due to the position dependence of \hbar . The changes resulting in the Euler-Lagrange equation, Newton's first and second laws, Newtonian gravity, and the Friedmann equation with a Cosmological Constant for the dominant path are shown and discussed. An attempt is made to explain the anomalous energy changes in the Earth flybys of six satellites in published data from the NASA Jet Propulsion Laboratory, which is considered to be an unsolved problem in physics, and a reasonable agreement is found with the model developed here for the Earth. The reported results of an experiment with tunnel diodes looking for Planck's constant variations is discussed in the context of the model, and an attempt is made to calibrate the model for the sun based on the latter. Parameters based on cosmological to planetary length scales are discussed, and also those based on the inspiral of masses emitting gravitational radiation.

Key Words: Planck's constant, Variable Planck's constant, non-Hermitian operators, Schrödinger Equation, Path Integral, Friedmann equation, Flyby Anomaly, Gravitational Waves.

1. Introduction

The possibility of the variation of fundamental constants would impact all present physical theory, while all reported variations or interpretations of data concluding a constant has varied are extremely controversial. Examples of work in this area include Dirac's Large Number Hypotheses [1], the Oklo mine from which could be extracted a variation of the fine structure constant [2,3], and the observations of quasars bounding the variation of the latter per year to one part in 10^{17} [4-6]. Recent theoretical work includes the impact of time dependent stochastic fluctuations of Planck's constant [7], and the changes with Planck's constant on mixed quantum states [8]. An authoritative review of the status of the variations of fundamental constants is given in [9].

Most physicists hold the position that any attempt to measure variations in dimensionful fundamental constants in isolation is physically meaningless. The succinct reasoning for examining a variable \hbar , here treated in isolation, is that its variation leads to forces that may be

compared to standard theory and noted measurement anomalies. Specifically, data pertaining to the Earth flybys of six satellites showing anomalous energy changes will be analyzed [34]. If an anomaly can be connected to the variation of a constant, then the “constant” is no longer by definition a constant, and it becomes meaningful to measure its change, replace it with new, correct constants that describe its variation, and augment physical theory based on the new phenomena. The anomalies will be treated as non-artifactual, real examples of energy non-conservation.

It is understood that the flyby anomaly has not been observed again in the very few flyby’s that have occurred since the publication of [34] in 2008. However, a rationale is given for why a variation in Planck’s constant may not be detectable in experiments with clocks to first order in [25], making the flyby anomaly a candidate to apply to the model of this paper to for calibration, and to infer a variation of Planck’s constant with, despite that the anomaly is not observed routinely. The flyby anomaly has not been explained in the dual sense of why it occurred in the first place, and then also why it is no longer being seen [38], leading to some to dismiss any work on the subject out of hand. An analysis has recently been conducted on the flyby of Juno past Jupiter, suggesting another possible anomaly observation [40].

Publicly available Global Positioning System (GPS) data was used to attempt to confirm the Local Position Invariance (LPI) of Planck’s constant under General Relativity [10-11]. LPI is a concept from General Relativity, where all local non-gravitational experimental results in freely falling reference frames should be independent of the location that the experiment is performed in. That foundational rule should hold when the fundamental physical constants are not dependent on the location. If the fundamental constants vary universally, but their changes are only small locally, then it is the form of the physical laws that should be the same in all locations.

The LPI violation parameter due to variations in Planck’s constant is called β_h . The fractional variation of Planck’s constant is proportional to the gravitational potential difference and β_h . The value found in [10] for variations in Planck’s constant was $|\beta_h| < 0.007$. This parameter is not zero, and is the largest of the violation parameters extracted in the study. The study did not report on the altitude dependence of Planck’s constant above the earth. A very recent study involving the Galileo satellites found that GR could explain the frequency shift of the onboard hydrogen maser clocks to within a factor of $(4.5 \pm 3.1) \times 10^{-5}$ [12], improved over Gravity Probe A in 1976 of $\sim 1.4 \times 10^{-4}$, these are the α_{rs} redshift violation values that may be compared to β_h .

Consistent sinusoidal oscillations in the decay rate of a number of radioactive elements with periods of one year taken over a 20 year span has been reported [13-18]. These measurements were taken by six organizations on three continents. As both the strong and weak forces were involved in the decay processes, and might be explainable by oscillations of \hbar influencing the probability of tunneling, an all electromagnetic experiment was conducted, designed specifically to be sensitive to Planck’s constant variations [19]. Consistent systematic sinusoidal oscillations of the tunneling voltage of Esaki diodes with periods of one year were monitored for 941 days. The tunnel diode oscillations were attributed to the combined effect of changes in the WKB tunneling exponent going as \hbar^{-1} , and changes in the width of the barrier going as \hbar^2 . The electromagnetic experiment voltage oscillations were correctly predicted to be 180 degrees out of

phase with the radioactive decay oscillations. This data can be made available for independent analysis by requesting it from the author of [19].

It is reasonable to suspect that the oscillations of decay rates and tunnel diode voltage are related to the relative position of the sun to the orbiting earth, and that there are resulting oscillations in Planck's constant due to position dependent gravitational effects, or effects with proximity to the sun. It should be mentioned that there have been studies in which it was concluded there was no gravitational dependence to the decay rate oscillations [20-21]. There is also dispute in the literature concerning the reality of the decay rate oscillations [22-24].

Either way, whether by gravitation or by some other mechanism, for the work to be presented, all that matters is that there be a position dependent \hbar , and it would be of value to understand the impact on the familiar formulations of the Feynman path integral, the Euler-Lagrange equation, Newton's laws, and Newtonian gravity. Findings from reference [25] will be used in the derivation, where frequency conservation in the Schrödinger equation as a means to retain Hermiticity was examined.

For the treatment of \hbar in this paper, and also in [25], it is important to emphasize is not as a dynamical field, and this leads to energy non-conservation. In another paper by this author, variations in \hbar are treated as a scalar dynamical field, coupling to fields through the derivative terms in the Lagrangian density [26], and the energy is shared between the fields. One of the solutions of [26] suggests that frequency may be a more fundamental dynamical variable than energy, leading to the idea of frequency conservation in [25], where it arises quite naturally. This paper concerns issues specific to the formalisms mentioned in a single-particle, non-field theoretic framework, however.

Variations in \hbar or any fundamental constant may be explainable by treatment as dynamical fields, but, they may not be, especially where the spatial dependence is concerned because there is so little experimental data on the subject. No one presently knows whether they actually are dynamical fields, or fixed background fields, or something else entirely, though much work has been done representing some of them as dynamical fields, with an emphasis on solving problems in cosmology: the Jordan-Brans-Dicke scalar-tensor theory with variable G developed in the late 1950's and early 1960's and note that G is dimensionful; Bekenstein models with variable fine structure constant, specifically the squared charge is varied, introduced in 1982 [27-28] where the emphasis was on the electromagnetic sector; the Cosmon of Wetterich with a field dependent pre-factor to the dynamical terms functioning somewhat like Planck's constant, falling to a constant value at high fields [29-30]; the investigations of Albrecht, Magueijo, Moffat, and Barrow on variable c used towards the explanation of the flatness, horizon, homogeneity, and cosmological constant problems [31-32, 41-42], where c^4 is made a dynamical field and is dimensioned.

Take for example,

$$\begin{aligned}
S_{GR} &= \int \left\{ \begin{aligned} &\frac{(c_o \mathbb{C})^4}{16G_o \pi} \xi R + \\ &\frac{(\hbar_o \psi)^2}{2} g^{\mu\nu} \nabla_\mu \psi \nabla_\nu \psi + \frac{(\hbar_o \psi)^2}{2} \frac{w}{\xi} g^{\mu\nu} \nabla_\mu \xi \nabla_\nu \xi + \frac{(\hbar_o \psi)^2}{2} g^{\mu\nu} \nabla_\mu \mathbb{C} \nabla_\nu \mathbb{C} \\ &+ \lambda \xi \psi \mathbb{C} R + L_m \{ \hbar, c, G \} \end{aligned} \right\} \sqrt{-g} d^4 x \\
\frac{\partial}{\partial x_o} &= \frac{1}{c_o \mathbb{C}} \frac{\partial}{\partial t} \\
c &= c_o \mathbb{C} \\
\hbar &= \hbar_o \psi \\
G &= G_o / \xi
\end{aligned} \tag{IIa-e}$$

Equation (IIa-e) shows in a single form an amalgam of possible couplings including a Jordan-Brans-Dicke-like scalar-tensor theory of alternative General Relativity with variable G , an Albrecht-Magueijo-Barrow-Moffat-like field for c , a field for \hbar like that of [26], which is different than the form of Bekenstein's for variable e^2 whose representative field squared divided the derivative terms. There is also the field theory of Modified Gravity (MOG) of Moffat, and the Tensor-Vector-Scalar (TeVeS) gravity of Bekenstein. There are many ways all the constants might be represented as fields, and many ways they might be coupled. Coupling fields together in this way is the accepted approach for the treatment of a constant, but is not the only possible approach, and here, something different will be tried.

As mentioned, the objective here is to formulate what the changes are to the most basic and familiar dynamical expressions in physics when \hbar varies spatially, conserving total frequency, not energy, following a logical course. The aforementioned anomalies will be examined [34], and relative to testing cosmological theories, the models of this paper would be experimentally testable by intentionally setting up more flyby orbits to be analyzed, or at least analyzing newly generated datasets from flybys as they become available, and by analyzing any orbital discrepancies of binary mergers emitting gravitational radiation.

2. The Altered Path Integral

The development to follow will depend on some prior results found in [25]. Equation (1) is the anticommutator-symmetrized Hermitian frequency-conserving operator controlling unitary time-evolution,

$$\hat{F}_\hbar = -\frac{1}{2m} \frac{1}{2} \{ \hbar(\vec{r}), \nabla^2 \} + \frac{V(\vec{r})}{\hbar(\vec{r})} = \frac{\hat{p}_\hbar^2}{2m} + V_\hbar(\vec{r}) \tag{1}$$

and the analog of momentum with units of $[\text{kg}\cdot\text{m}/\text{s}/\hbar^{1/2}]$ is,

$$\hat{p}_h = \frac{1}{i} \sqrt{\frac{1}{2} \{ \hbar(\bar{r}), \nabla^2 \}} \quad (2)$$

Equations (1-2) were derived for the condition that \hbar had no explicit time dependence. The completeness operator in the position representation that will result in summation over every possible path at each time-slice is,

$$\int dx_j(t_j) |x_j, t_j\rangle \langle x_j, t_j| = 1 \quad (3)$$

Using (3) by repeated insertion N times (for N time slices) between the brackets of the transition amplitude for a particle initially at (x_i, t_i) to be found at (x_f, t_f) , one may write for the amplitude,

$$\langle x_f, t_f | x_i, t_i \rangle = \int \prod_{j=1}^{N-1} dx_j(t_j) \prod_{k=0}^{N-1} \langle x_{k+1}, t_{k+1} | x_k, t_k \rangle \quad (4)$$

The completeness operator will be needed for the equivalent of the momentum representation to be used,

$$\int dp_h |p_h\rangle \langle p_h| = 1 \quad (5)$$

A general amplitude in (4) will now be examined. Using the time evolution operator followed by approximation to first order,

$$\begin{aligned} \langle x_1, t_o + \Delta t | x_o, t_o \rangle &= \langle x_1 | \exp(-i\hat{F}_h \Delta t) | x_o \rangle \\ &\approx \langle x_1 | \exp\left(-i \frac{\hat{p}_h^2}{2m} \Delta t\right) \exp(-iV_h(\hat{x})\Delta t) | x_o \rangle \end{aligned} \quad (6)$$

Inserting (5) into (6) and acting with the operators,

$$\begin{aligned} \langle x_1, t_o + \Delta t | x_o, t_o \rangle &= \int dp_h \langle x_1 | \exp\left(-i \frac{\hat{p}_h^2}{2m} \Delta t\right) | p_h \rangle \langle p_h | \exp\left(-i \frac{V(\hat{x})}{\hbar(\hat{x})} \Delta t\right) | x_o \rangle \\ &= \int dp_h \langle x_1 | p_h \rangle \langle p_h | x_o \rangle \exp\left(-i \frac{p_h^2}{2m} \Delta t\right) \exp\left(-i \frac{V(x_o)}{\hbar(x_o)} \Delta t\right) \end{aligned} \quad (7)$$

The two needed p_h eigenfunctions, with factors of $\hbar^{1/2}$ dividing the exponent to produce the right units for the approximate basis become,

$$\begin{aligned}\langle p_h | x_o \rangle &\approx \frac{\exp\left(-ip_h x_o / \sqrt{\hbar(x_o)}\right)}{\sqrt{2\pi\hbar(x_o)}} \\ \langle x_1 | p_h \rangle &\approx \frac{\exp\left(ip_h x_1 / \sqrt{\hbar(x_1)}\right)}{\sqrt{2\pi\hbar(x_1)}} \approx \frac{\exp\left(ip_h x_1 / \sqrt{\hbar(x_o)}\right)}{\sqrt{2\pi\hbar(x_o)}}\end{aligned}\quad (8a-b)$$

The approximate basis above is justified in [25] where it was shown that for a mild enough gradient in \hbar , the free-particle wavefunctions are approximately planewaves, and the Ehrenfest theorem relating the position expectation value time derivative to the momentum is exactly retained. The approximation will break down if the gradient becomes too large, and will become important in the analysis to follow of the sun. Substituting (8a-b) into (7) and (6) and integrating,

$$\begin{aligned}\langle x_1, t + \Delta t | x_o, t_o \rangle &= \int \frac{dp_h}{2\pi\hbar(x_o)} \exp\left(-i\left\{\frac{p_h(x_o - x_1)}{\sqrt{\hbar(x_o)}} + \left(\frac{p_h^2}{2m} + \frac{V(x_o)}{\hbar(x_o)}\right)\Delta t\right\}\right) \\ &= \frac{1}{2\hbar(x_o)} \sqrt{\frac{m}{2\pi i \Delta t}} \exp\left(\frac{i}{\hbar(x_o)} \left\{\frac{1}{2} m \underbrace{\left(\frac{x_1 - x_o}{\Delta t}\right)^2}_{\dot{x}_o^2} - V(x_o)\right\} \Delta t\right)\end{aligned}\quad (9)$$

The term in the curly brackets of (9) is the classical Lagrangian L_c , now divided by the position dependent \hbar ,

$$\langle x_1, t_1 | x_o, t_o \rangle = \frac{A}{\hbar(x_o)} \exp\left(i \frac{L_c(x_o)}{\hbar(x_o)} \Delta t\right)\quad (10)$$

Now substituting (10) into (4), taking the limit $N \rightarrow \infty$, and passing the resulting sum in the exponent to an integral, the new form of the path integral is,

$$\begin{aligned}\langle x_f, t_f | x_i, t_i \rangle &= \int D_h x(t) \exp\left(i \int \underbrace{\frac{dt}{\hbar(x(t))}}_{d\tau(x)/\hbar_x} L_c(x(t), \dot{x}(t))\right) \\ D_h x(t) &= \lim_{N \rightarrow \infty} \prod_{j=1}^{N-1} A \frac{dx(t_j)}{\hbar(x(t_j))}\end{aligned}\quad (11a-b)$$

Normally, the \hbar that appears in the denominator of the exponent is a constant, but in (11) it is not, and is being integrated. The complication of the product $1/\hbar(x_j)$ in the pre-factor of (11) appears in $D_h x(t)$, but is not important in what follows.

Equation (11a) has been written to provide an interpretation for what a variation in Planck's constant means – it is related to variations in the rate of time passage over the classical path, which must be made stationary in combination with the Lagrangian as part of the action. Once made stationary, there are resulting detectable forces.

3. Euler-Lagrange Equation for Dominant Path and Total Frequency Conservation

The usual argument is to say that the classical path is the one that makes the classical action in the exponent of the path integral stationary, all other paths cancelling by rapid oscillations in the limit that the constant $\hbar \rightarrow 0$. That will still be the case if the entire function \hbar in (11) goes to zero.

To be more precise, the classical trajectory is recovered from the path integral when the classical action is much larger than the constant \hbar , due to mass or energies becoming large.

Let a different question be posed. The “dominant path” will be used to refer to one that makes the integral in the exponent of (11) stationary. The trajectories around the dominant path are systematically different from the true classical path due to the variation of \hbar . What may be expected?

To answer that, the condition for a stationary exponent in (11) in terms of generalized coordinates is given by a modified form of the Euler-Lagrange equation,

$$L = L(\underbrace{q_1(t), q_2(t), q_3(t)}_{q_i}, \underbrace{\dot{q}_1(t), \dot{q}_2(t), \dot{q}_3(t)}_{\dot{q}_i})$$

$$\hbar = \hbar(q_1(t), q_2(t), q_3(t))$$

$$\frac{d}{dt} \frac{\partial(L_c / \hbar)}{\partial \dot{q}_i} - \frac{\partial(L_c / \hbar)}{\partial q_i} = 0$$

$$\frac{d}{dt} \frac{\partial(L_c / \hbar)}{\partial \dot{q}_i} = \frac{d}{dt} \left(\overbrace{\frac{1}{\hbar} \frac{\partial L_c}{\partial \dot{q}_i} - \frac{L_c}{\hbar^2} \frac{\partial \hbar}{\partial \dot{q}_i}}^{p_i} \right) = \frac{1}{\hbar} \frac{d}{dt} \frac{\partial L_c}{\partial \dot{q}_i} - \frac{1}{\hbar^2} \frac{\partial L_c}{\partial \dot{q}_i} \underbrace{\sum_j \frac{\partial \hbar}{\partial q_j} \dot{q}_j}_{\bar{\nabla} \hbar \cdot \dot{\vec{q}}}$$

$$\frac{\partial(L_c / \hbar)}{\partial q_i} = \frac{1}{\hbar} \frac{\partial L_c}{\partial q_i} - \frac{L_c}{\hbar^2} \frac{\partial \hbar}{\partial q_i}$$

(12a-f)

$$\frac{d}{dt} \frac{\partial L_c}{\partial \dot{q}_i} - \frac{\partial L_c}{\partial q_i} = (\bar{\nabla} \ln \hbar \cdot \dot{\vec{q}}) \frac{\partial L_c}{\partial \dot{q}_i} - L_c \frac{\partial \ln \hbar}{\partial q_i}$$

The left side of (12f) are the usual Euler-Lagrange terms, but the right that is usually zero is no longer. The classical equation of motion is recovered when the logarithmic derivative of \hbar

vanishes. In the absence of an external potential, classical conjugate momentum p_{ic} and modified conjugate momentum p_i are not conserved due to the position dependence of \hbar .

Equation (13) shows that the total frequency $W = H_c/\hbar$ is conserved and not the total classical energy. Taking the total time derivative of L_c/\hbar and using (12c),

$$-\frac{\partial(L_c/\hbar)}{\partial t} = \frac{d}{dt} \left(\sum_i \dot{q}_i \frac{\partial(L_c/\hbar)}{\partial \dot{q}_i} - L_c/\hbar \right) = \frac{d}{dt} \frac{H_c}{\hbar} = \frac{dW}{dt} = 0 \quad (13)$$

For a conserved W , on any trajectory in which the value of \hbar is equal at the start and end, the total energy is restored, though not conserved.

4. Newton's First and Second Law for Dominant Path

From (12f), the equation of motion for the path that makes (11) stationary is a modified Newton's second law,

$$m\ddot{\vec{x}} = -\bar{\nabla}V_c + m(\bar{\nabla} \ln \hbar \cdot \dot{\vec{x}})\dot{\vec{x}} - (\bar{\nabla} \ln \hbar) \left(\frac{1}{2} m |\dot{\vec{x}}|^2 - V_c \right) \quad (14a-b)$$

$$m\ddot{x} = F_c + \frac{\partial \ln \hbar}{\partial x} H_c$$

where (14a-b) are in 3-D and 1-D, respectively. $H_c = T_c + V_c$ is the classical total energy, and can be written as (14b) only in 1-D. With no external potential, the equation (14b) becomes,

$$\ddot{x} = \frac{\partial \ln \hbar}{\partial x} \left(\frac{1}{2} \dot{x}^2 \right) \quad (15)$$

From Equation (15), if the particle is at rest, it stays at rest, per the first half of Newton's first law. For the second half of Newton's first law, it is found that a particle in motion tends to accelerate or decelerate, depending on the functional form of \hbar . Therefore, momentum is not conserved.

Assuming the logarithmic derivative of \hbar is a constant k , one finds,

$$\hbar = \hbar_0 e^{kx}$$

$$x(t) = -\frac{2}{k} \ln \left(\frac{c_1 + kt}{c_2} \right) \quad (16a-d)$$

$$\dot{x}(t) = -\frac{2}{c_1 + kt}$$

$$\ddot{x}(t) = \frac{2k}{(c_1 + kt)^2}$$

From (16c), one sees that once in motion, the particle can never be at rest unless an infinite amount of time has passed. The acceleration may increase, or decrease depending on the sign of k . In Figure 1, Equations (16b-c) are plotted for $k=\pm 1$, and $c_1=c_2=1$ arbitrary unit.

An object initially moving in the direction of lower Planck's constant decelerates asymptotically to zero velocity, but never fully stops. If it is initially moving towards higher Planck's constant, it accelerates in that direction to infinite velocity, where after the position becomes undefined.

Clearly, the classical energy is no longer conserved, as there is a tendency for matter to receive an added push through space in the direction of increasing \hbar at the gentlest disturbance from rest in that direction, for large $|k|$.

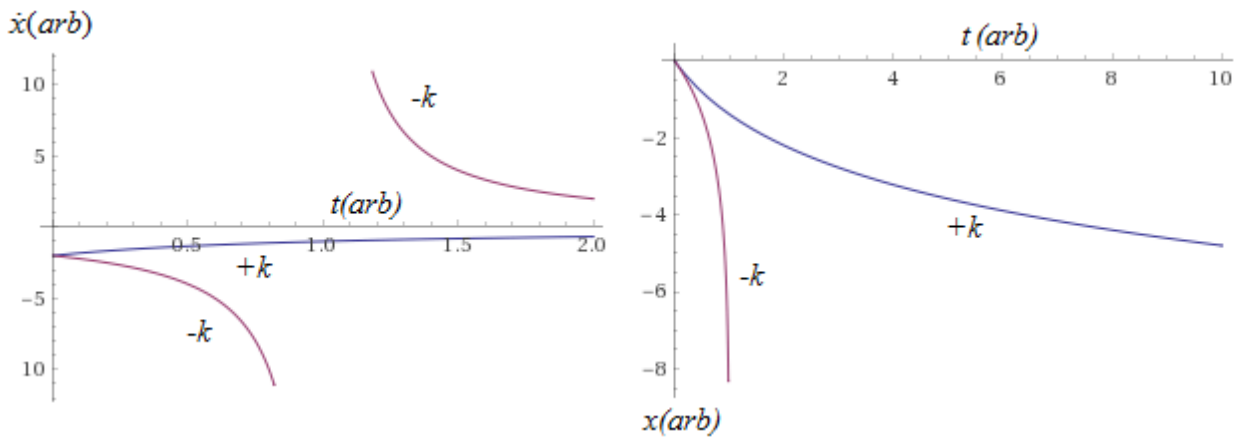


Figure 1a. (Left) Velocity as a function of time. (Right) Position as a function of time.

5. Newtonian Gravity for Dominant Path (NGDP)

From (14a), for a mass m in a gravitational potential caused by M ,

$$\begin{aligned}
 m\ddot{\vec{x}} &= -\frac{GMm}{|\vec{x}|^2} \hat{x} + m(\bar{\nabla} \ln \hbar \cdot \dot{\vec{x}}) \dot{\vec{x}} - (\bar{\nabla} \ln \hbar) \left(\frac{1}{2} m |\dot{\vec{x}}|^2 + \frac{GMm}{|\vec{x}|} \right) \\
 m\ddot{r} &= F = -\frac{GMm}{r^2} + \partial_r \ln \hbar \left(\frac{1}{2} m \dot{r}^2 - \frac{GMm}{r} \right) \\
 r_o &= -\frac{1}{\partial_r \ln \hbar(r_o)} > 0 \\
 \frac{v_o^2}{2} &= -\frac{1}{\partial_r \ln \hbar} \frac{GMm}{r^2} - \frac{GMm}{r}
 \end{aligned} \tag{17a-d}$$

where (17b) is for the situation with no velocity other than radial, and a radially dependent \hbar . It is possible now for the particle to remain at rest in the gravitational field, which is normally not possible except infinitely far away from M . It will be so if placed at zero velocity at a radius equal to (17c). For the solutions presented, Equation (26b), it can be shown that $r_o = 0$ and ∞ are

the only values admitted. There is also a tangential velocity to the gradient at which the total radial force goes to zero, v_o , Equation (17d).

6.0 Model Parameterization at Different Scales

The NGDP model offers a new degree of freedom that may be applied to behavior at varying length scales. There may be interactions between the behaviors at varying length scales, where that of a longer length scale sets an overall trend that the smaller length scale behavior is superimposed on.

6.1 Galactic Scale Parameters: Galaxy Rotation Curves and Dark Matter

It is possible to find a profile of \hbar that would lead to the flattening of a galaxy rotation curve without dark matter with NGDP, although it requires a large variation in \hbar , and this will be shown. From (14a) for a radially dependent \hbar , a general radially dependent classical potential energy V_c and a velocity v perpendicular to the gradient, the total force is radial. V_c is general, and it can contain the potential energy of multiple distributions of matter (luminous, dark, and point-like). The term v_n is the net velocity from all matter, and v is the measured velocity. Set equal to the centripetal force for a circular orbit, the velocity may be solved for, producing (18a-d). Setting the velocity to be a constant independent of radius per a perfectly flat rotation curve of infinite range, one may solve for the profile using (18a-d). To find values to insert, the rotation curve is computed for a dark matter containing galaxy, using the values of $M = 1.3 \times 10^{11}$ solar masses for all the visible stars in the galaxy, and a dark matter halo of 1.5×10^{12} solar masses, where at a distance of 60 kpc the velocity is about 150 km/s, and flattening out. No point mass for the black hole is used, as it does not impact the rotation curve in the outer points of the galaxy. Then, using the latter values for v , and M with $\phi_c = -GM/r$ but without the mass of the dark matter, it is found that in order to maintain the constant velocity, \hbar would have to decrease by a factor of 0.755 over 10-60 kpc reaching a minimum mid-range, using (18d). The required mid-range minimum becomes a factor of 0.9 for $M = 9 \times 10^{10}$ solar masses over 10-30 kpc. This is the simplest approximation for a star near the edge of the galaxy, and illustrates that a minimum can result.

While more realistic simulations with actual non-dark matter density profiles and real rotation curves may reduce the required change in \hbar , it is not likely to be small, and would be problematic for fusion in most of the stars in the flat velocity region. A reason was given in [25] for why experiments with clocks (and hence the frequency of light) would not, to first order, reveal a change in \hbar , and it is due to the proposed conservation of total frequency instead of total energy. The spatial variation would be revealed in the motion of gravitationally interacting bodies and light lensing in that case. However, the large variation needed, and the issue with fusion in the stars, prompts the conclusion that the galaxy rotation curves could not be explained by this mechanism directly and alone. The needed variation in \hbar can be reduced if the impact of a varying \hbar works in tandem with dark matter, shown in Equations (18c-d) and Figure 1b.

Consider an alternative starting point for the explanation of the nature of dark matter. The stars are seen because of a combination of gravitational heating, and fusion via tunneling, which becomes more difficult if \hbar is smaller, but also, the strengths of all the known forces dependent

on \hbar would be altered. If the galactic-scale trend in Planck's constant suppressed fusion and other normal quantum mechanical interactions via known forces in most of the matter in the galaxy, most of it would be dark (or at least less luminous), but would be gravitationally active. The galactic-scale variation of Planck's constant would then be limited to that necessary to prevent fusion and the other expected interactions. Then, local variations near stars could raise Planck's constant so some matter may fuse and normally interact, and that is what is luminous. The combination of the non-fusing matter and the added force from the derivative in Planck's constant could together explain the rotation curves, and simultaneously explain why most of the matter is dark, and why it can only interact gravitationally.

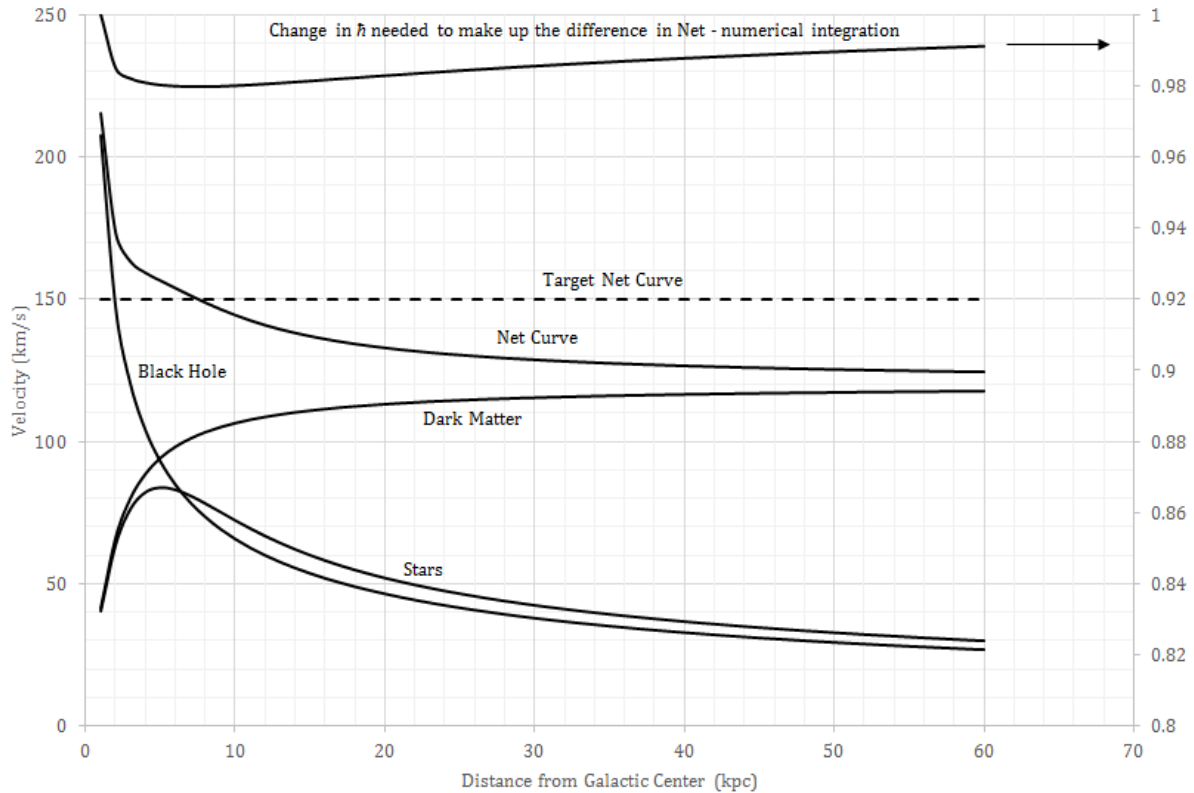


Figure 1b. Depression in Planck's constant in the vicinity of a galaxy. The numerical integration of the net velocity curve to produce ϕ is good up to a constant of integration ϕ_0 , which must be negative. The r_1 value where the fraction of Planck's constant falls from unity is set at 1 kpc.

For NGDP, there would not be a MOG-, TeVeS-, or MoND-like explanation of the rotation curves without dark matter, as it is still needed, working in concert with $\partial \ln \hbar$. The analysis of the flyby anomaly will show that \hbar needs to increase approaching the focus of an orbit, and provides a rationale for why there could be local spikes in \hbar . It is also pointed out in [25] that the wavefunctions of particles increase in amplitude in regions of lower \hbar , so particles with mass can gather probabilistically, providing an alternative rationale for why there are massive particles accumulating around galaxies forming a halo. As an exaggerated example, consider Figure 1b, where an ideally flat rotation curve is sought. With a star matter density profile, reduced dark matter density profile, and a black hole mass, it is possible to find a solution in which a minimum

forms in \hbar , which per [25] would increase the amplitude of single particle wavefunctions in the vicinity.

$$\begin{aligned}
v^2(r) &= \frac{-\partial_r V_c + V_c \partial_r \ln \hbar}{-\frac{m}{r} + \frac{m}{2} \partial_r \ln \hbar} \\
\partial_r \varphi_c &= \frac{v_n^2(r)}{r} \\
\varphi_c &= \int \frac{v_n^2(r)}{r} dr + \varphi_o \leq 0 \\
\partial_r \ln \hbar &= \frac{\frac{v^2(r)}{r} - \partial_r \varphi_c}{\frac{1}{2} v^2(r) - \varphi_c}
\end{aligned} \tag{18a-d}$$

The inclusion of more dark matter necessitates a smaller change in \hbar . Both the probability of fusion, and the residual strong force, contain factors of $\exp(-C/\hbar)$. The following must be elucidated in a mutually consistent way that constrains the possible solutions:

1. How much smaller \hbar needs to become to shunt fusion, and other forces.
2. Whether the concentration of the wavefunctions of massive particles in the depression in \hbar can be made consistent with the required amount of dark matter.
3. Finding unique solutions of \hbar . With conditions (1) and (2) not participating, for any fixed set of matter distributions, the solutions for \hbar are non-unique, as the radius r_1 set for the fraction of \hbar to vary from unity, and the constant φ_o both alter the \hbar profiles, but still produce the target curve.

6.2 Cosmological Scale Parameters: Newtonian Derivation of Friedmann Equation for Dominant Path and the Cosmological Constant

A connection of the path integral derivation above has not been made with general relativity, although its form may be that of Equation (32). In the absence of a higher theory for a total frequency-conserving version of the Einstein field equations, it is possible to derive an expression for the Friedmann equation using Newtonian gravity, following a procedure outlined in Liddle [33], adapted to include features of NGDP. Since the Lagrangian L_c/\hbar is in terms of frequency and not energy, the Hamiltonian is also, is total frequency conserving as there is no explicit time dependence, and was called W ,

$$W = \frac{H_c(r)}{\hbar(r)} = \frac{1}{\hbar(r)} \left(\frac{1}{2} m \dot{r}^2 - \frac{GMm}{r} \right) = \frac{1}{\hbar(r)} \left(\frac{1}{2} m \dot{r}^2 - \frac{4\pi G \rho r^2}{3} \right) \tag{19}$$

Equation (19) describes the frequency of a particle of mass m at a radius r from the origin of a homogeneous mass distribution of density ρ . Changing to the co-moving coordinates x in terms of the scale factor a ,

$$r(t) = a(t)x \quad (20)$$

Making this substitution, multiplying both sides by $2/ma^2x^2$, it is found that,

$$\left(\frac{\dot{a}}{a}\right)^2 = \frac{8\pi G}{3}\rho + \frac{2W}{ma^2x^2}\hbar(ax) \quad (21)$$

The second term of (21) must be independent of x in order to maintain homogeneity. There are a number of ways this might be accomplished. One way will be examined that produces a term like the cosmological constant. In the usual derivation, the energy of a particle is constant, but changes with separations as $U \propto x^2$, to allow a connection to be made to the curvature k , and to arrive at the same form of expression derived from general relativity. Let it be assumed this persists in the conserved frequency as $W \propto x^2$, and that the variation of \hbar has a similar dependence. Since \hbar must have no explicit time dependence at a separation r , using one of the solutions found in [26] for the functional form of \hbar shown in Equation (26) below,

$$\hbar = \hbar_o + f_h(ax) = \hbar_o + b(ax)^2 \quad (22)$$

$$\left(\frac{\dot{a}}{a}\right)^2 = \frac{8\pi G}{3}\rho + \frac{2W\hbar_o}{ma^2x^2} + \frac{2Wf_h(ax)}{ma^2x^2} \quad (23)$$

Rewriting (23) using $kc^2 = -2W\hbar_o/mx^2$,

$$\left(\frac{\dot{a}}{a}\right)^2 = \frac{8\pi G}{3}\rho - \frac{kc^2}{a^2} - \frac{kc^2}{\hbar_o} \frac{f_h(ax)}{a^2} \quad (24)$$

It is seen from (24) that another term enters the usual Friedmann equation. Provided that f_h/a^2 is sufficiently constant and negative, the additional term could serve as the cosmological constant. The factor f_h is not written as $f_h(a)$ without x , because then it would have explicit time dependence, which was not the condition under which (1), (2) and (12) were derived.

From (22) the universe is still isotropic, as a quadratic change in \hbar is seen in every direction. As there is no single origin of x , the universe is still homogeneous in the sense that at one specific position an observer concludes that \hbar is multi-valued, seeing the same distribution of \hbar values from every other position when treated as the origin. The issue is not homogeneity, but the multiple values. The problem is mitigated if what one actually observes is the average of all possible values. Averaging (22) and (24) over the co-moving coordinates, only the last term is affected by the averaging, from which follows,

$$\begin{aligned}
\langle x^2 \rangle_x &= \frac{\pi^2 - 4}{2} x_R^2 \sim \frac{\pi^2 - 4}{2} \frac{1}{k} \\
\langle \hbar \rangle_x - \hbar_o &= \langle f_{\hbar}(ax) \rangle_x = \langle ba^2 x^2 \rangle_x = ba^2 \langle x^2 \rangle_x \sim \frac{\pi^2 - 4}{2} \frac{ba^2}{k} \\
\frac{\Lambda}{3} &= -\frac{kc^2}{\hbar_o} b \langle x^2 \rangle_x \sim -\frac{\pi^2 - 4}{2} \frac{bc^2}{\hbar_o} \\
\hbar &\sim \hbar_o \left(1 - \frac{2\Lambda}{3(\pi^2 - 4)c^2} r^2 \right) \\
\langle \hbar \rangle_x &= \hbar_o \left(1 - \frac{\Lambda}{3} \frac{a^2}{kc^2} \right) \tag{25a-e}
\end{aligned}$$

$$\begin{aligned}
\Lambda &= 9.95 \times 10^{-36} [1 / s^2] \\
|b| &\leq 1.324 \times 10^{-87} [Js / m^2] \\
r_o &\sim 2.822 \times 10^{26} [m]
\end{aligned}$$

From the second term of (25c), in order for there to be a non-zero and positive cosmological constant, $k \neq 0$ so that the universe could not be perfectly flat, but instead open or closed. If it is closed, the average value of x^2 over x would be finite and also be a constant, and then necessarily $b < 0$.

To go farther than this, another identification must be made. Evaluating the average (25a) using a spherical surface of radius x_R , there is a resulting factor of x_R^2 by that example, and so the average of x^2 is identified with $1/k$, from which the last terms of (25a,b,c) are derived. The geometrical factor that results will be used for the order of magnitude estimates, though (25e) is independent of it. One sees explicitly from the last term of (25b) that since b must be zero if the universe is perfectly flat, the cosmological constant would be zero. From the last term of (25a), the \hbar that is measured falls with time and can eventually become zero, and also negative.

The measured value $\langle \hbar \rangle_x \leq \hbar_o$, so an upper limit on the absolute value of b can be estimated from (25c) using the measured value. From (25d) the separation r_o is that where Planck's constant would fall to zero *before averaging* - remarkably on the same order as the radius of the present-day observable universe.

6.3 Planetary Scale Parameters: The Earth Flyby Anomaly

The behavior expressed in the most fundamental equations in physics for the dominant path certainly does not describe behavior witnessed every day. None of the equations here conserve energy, rather, total frequency. Evidence of non-conservation of energy in a classical system may be relatable to the effects described here, and more examples need to be found.

Consider Equation (13) and conservation of the total frequency W . If infinitely far from a potential's center, should \hbar fall to a constant and the potential to zero, then a moving body's total energy would be equal at the extreme distances, but not between when closer to the center. That is, energy would be "restored" but not conserved. Therefore, when a measurement is made of the moving bodies velocity and position when not infinitely far from the center on a hyperbolic trajectory, a non-energy conserving anomaly will be shown in the extracted osculating excess hyperbolic velocity $V(\infty)$, and it can only be seen if the analysis is done on data specifically not taken at effectively infinite ranges, with a radial asymmetry about the center. It is emphasized the latter is not seen in normal Newtonian gravity.

In NGDP on a hyperbolic trajectory, the greater the range, the greater the percentage of restored energy, and the less anomalous the energy change will appear. Also, the more symmetric the analysis about the center, the less anomalous the energy difference will appear.

Parameters for the Earth for the variation of Planck's constant will now be extracted from an analysis of the flyby anomaly, with all trajectories starting and terminating at equal time. It is understood that the range chosen for the analysis will impact the extracted parameters. Though an analysis may show energy conservation at symmetric terminal points along a trajectory, or at effectively infinite range, the position as a function of time will differ from Newtonian gravity, and this is why the full trajectory dataset is needed for a proper parameter extraction. All these points will be demonstrated. That the anomaly can be made to go away depending on when the analysis along the trajectory is done offers an explanation as to why the anomaly is no longer seen, or may not been seen routinely.

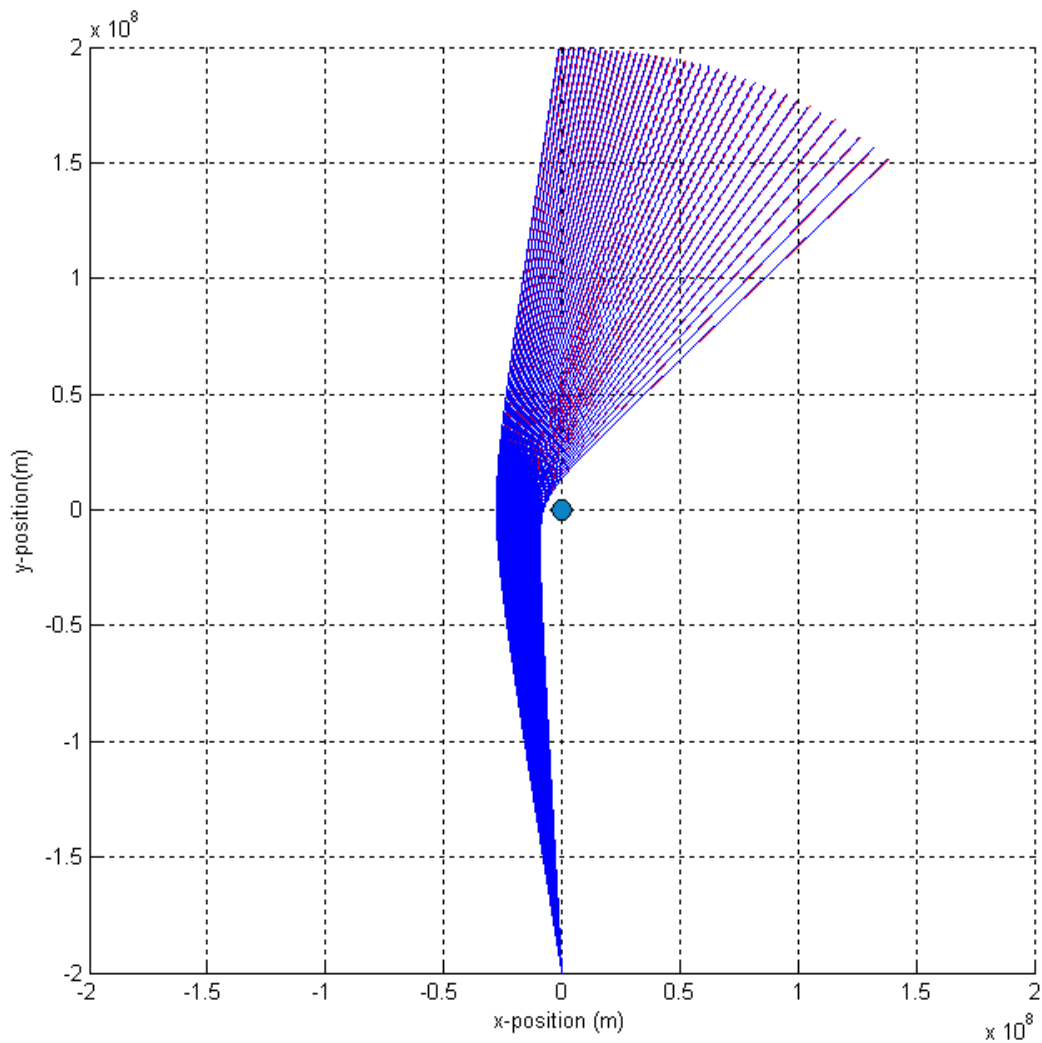


Figure 2. Trajectory of NGDP (blue) per Equations (17a) and (26d). Normal gravity is also shown (red). The total velocity is fixed at 9 km/s, and the x-velocity ranges from -0.5 to -1.42 km/s producing the trajectory fan. The Earth is the green circle, the equator is the x-axis. The leftmost trajectory has a starting x-velocity of -1.42 km/s, for which the asymptotic velocity change is zero.

The flyby anomaly is described in a paper from the Jet Propulsion Laboratory. It describes anomalous changes in the orbital energy in the Earth flybys of six satellites [34]. The energy non-conservation was on the order of one part in 10^6 , and was fit by an empirical formula. No physical explanation was found in the investigation. If the detailed orbital trajectory data as a function of position and time were available, and it is not presently, Equation (14a) or (17a) could be used for trajectory analysis. Using Equation (17a) and (26a-e) derived in [25-26], one can compute the trajectories of masses in flyby orbits. The spatial solution for \hbar has an infinite number of terms and was derived from principles outlined in [26], and they are the classical vacuum solutions of a massless zero-momentum field. There is no mass or gravity involved in the derivations. The solutions were,

$$\left(\frac{\hbar(r)}{\hbar_\infty}\right)^2 = \sum_{l=0}^{\infty} \sum_{m=0}^{\infty} (A_l r^l + B_l r^{-l-1}) P_l^m(\cos \varphi) (S_m \sin(m\theta) + C_m \cos(m\theta)) \quad (26a-b)$$

$$\left\langle \left(\frac{\hbar(r)}{\hbar_\infty}\right)^2 \right\rangle_{\varphi}^{m=0} = \sum_{l=0}^{\infty} (A_l r^{2l} + B_l r^{-2l-1}) \rightarrow 1 + \frac{b_4/b_3}{r} + \sum_{l=1}^{\infty} B_l r^{-2l-1}$$

The forms used for fitting will be based on (26a-b), with some additional features, and with the understanding that the values of the function are very close to unity,

$$\frac{\hbar(r)}{\hbar_\infty} \rightarrow \begin{cases} \sqrt{1 + \left(\frac{b_4/b_3}{r} + \sum_{l=1}^{\infty} B_l r^{-2l-1}\right) f(r)} & r \geq r_h \\ \frac{\hbar(r_h)}{\hbar_\infty} & r < r_h \end{cases}$$

$$\partial_{x,y,z} \ln \hbar = \begin{cases} \frac{1}{2} \frac{(x,y,z)}{r} \left(\frac{\hbar_\infty}{\hbar(r)}\right)^2 \left(f(r) \left(-\frac{b_4/b_3}{r^2} - 3\frac{B_1}{r^4} - 5\frac{B_2}{r^6} - 7\frac{B_3}{r^8} + \dots \right) + \frac{\partial f(r)}{\partial r} \left(\frac{b_4/b_3}{r} + \sum_{l=1}^{\infty} B_l r^{-2l-1} \right) \right) & r \geq r_h \\ 0 & r < r_h \end{cases} \quad (26c-e)$$

$$f(r) = \frac{1}{e^{(r-a)/s} + 1}$$

Although not a set of orthogonal functions forming a basis, a large range of profiles, symmetries or lack thereof can be addressed. Averaging over angular dependences may be performed to develop a pure radial dependence, as there are no constraints pinning the solution to any particular orientation or weighting. For example, with azimuthal symmetry $m=0$, the Associated Legendre Polynomials become just the Legendre Polynomials P_l , and averaging from $\varphi = 0$ to π will leave the even l terms non-zero – this is the same as eliminating the angular dependence per (26b), written so that l can be odd or even. Also, only the solutions going to zero at infinite range are kept. An ad-hoc decay function $f(r)$ is added to the expressions to prevent interference with the orbits of other bodies at greater range. For example, a function resembling the Fermi-Dirac distribution, per (26e) might be used. Neither the clipping at close range below r_h , or the decay at greater range were derived from a theory.

At this time the author is not able to numerically simulate all of the very fine deviations and details in the orbital trajectories reported in [34] to a precision matching the capability of the Jet

Propulsion Laboratory, which includes general relativity and many other effects. However, Equations (17a) with various terms of (26d) are numerically integrated in Matlab in what is to follow. All of the Matlab scripts and functions will be made available upon request from this author for independent analysis.

For satellite trajectories with velocities and distances about the Earth similar to those reported in [34], Equations (17a) and (26d) are capable of producing energy changes on the flyby. The calculation done here is very simple, and does not use the exact orbits of [34]. The intention is to demonstrate generally how such behavior as noted by Anderson can come about. The flyby orbits of Figure 2 are set up, the x-velocity of the starting point is swept over a range, and the orbit is computed numerically for each of the starting x-velocities, with all other parameters fixed. The initial and final velocities at the start and end of the trajectories $V(r)$ are converted to the osculating element asymptotic velocities $V(\infty)$ using (27d) for a hyperbolic orbit, and the fractional differences between $\Delta V(\infty)/V(\infty)$ are computed, along with the incoming and outgoing orbital velocity declination angles at the start and ends of the trajectory approximating infinity as $\delta^{i,o} = \tan^{-1}(V_y^{i,o} / V_x^{i,o})$. With no Earth rotation in the model, the initial and final asymptotic velocities should be equal with normal gravity due to energy conservation, and there should be a delta with the NGDP due to energy non-conservation. For the negative values of the delta, the simulation is run from the ending point of the forward simulation, but with negative velocities (or backward), which proved to produce results very close to the negative values of the forward simulation for several trial points. Therefore, the backward simulation is just the negative of the forward simulation, and that is what is shown in Figure 3a-b. The calculation is repeated for normal gravity for each x-velocity, and changes in the relative asymptotic velocity delta are subtracted from the curve for the NGDP. That is, the delta in relative asymptotic velocity resulting when there is normal gravity is the numerical background error that is subtracted off of the NGDP delta, Figure 3e. A sensitivity analysis was performed, reducing the time step by factors of ten in the numerical solution of the differential equations, until showing: 1) solution curves that overlay the data of [34] without changing; 2) a nearly flat numerical background.

The calculation has also been done without the conversion to the osculating element $V(\infty)$ using (27d) at the beginning and end of the trajectory. This had little impact on the agreement of the model with the Anderson data, but it does increase the numerical background greatly, and so the conversion is employed.

There is no Earth rotation, and therefore no equator inherent in the model. The equivalent of the equator in this model is found by changing the x-velocity in normal gravity, until the velocity delta is minimized, and incoming and outgoing declination angles are symmetric about some axis. That axis turns out just to be parallel to the x-axis bisecting the Earth, Figure 2.

The authors of [34] fit their data to an empirical function of the form,

$$\frac{\Delta V(\infty)}{V(\infty)} = K (\cos \delta^i - \cos \delta^o)$$

$$|\delta^i| \leq |\delta^o| \rightarrow \Delta V(\infty) \geq 0 \tag{27a-d}$$

$$K = 3.099 \times 10^{-6} = \frac{2v_E}{c}$$

$$V(\infty) = \sqrt{V^2(r) - 2GM/r}$$

where $V(\infty)$ is the asymptotic velocity expected on a hyperbolic trajectory, $\Delta V(\infty)$ is the anomalous additional velocity, and δ^i and δ^o are the incoming and outgoing asymptotic velocity declinations of the flyby. The equatorial velocity of the Earth is $v_E = \omega_E R_E$, and the constant is found empirically, not from a theory, though has the form of twice the factor appearing in the low-speed Doppler shift $\Delta f/f \approx v/c$. Mbelek provides a derivation of this formula based on both the transverse Doppler effect and time dilation in special relativity, and concludes that the reported anomaly is not an actual energy gain of the craft, rather only appears as one due to the unaccounted for effect in the ground-based tracking [37]. Equation (27d) is the asymptotic velocity at infinity extracted from a known velocity and radius for a hyperbolic trajectory. The value of K when plotting the Anderson data was found by this author to be 3.14×10^{-6} with an $R^2 = 0.998$, not the value reported of 3.099×10^{-6} reported.

Figure 3a shows all of the data of reference [34] plotted against the modeling results of a six-parameter fit. In order to be consistent with the definition of a declination angle restricted to $\pm 90^\circ$ above and below the x-axis and to get the sign of the slope correct, positive values of the leading term b_4/b_3 must be used. The positive values mean that \dot{h} must increase approaching the orbit focus. The total fixed velocity of the simulations used was 9 km/s, and from -0.5 to -1.42 km/s in the x-direction, in the range of [34]. The six-parameter representation of \dot{h} using $[b_4/b_3, B_1, B_2, B_3, B_4, r_h] = [6 \times 10^4 \text{ m}, -6 \times 10^{18} \text{ m}^3, 1.5 \times 10^{32} \text{ m}^5, -4 \times 10^{45} \text{ m}^7, 2.5 \times 10^{59} \text{ m}^9, 1.628 \times 10^7 \text{ m}]$ is shown in Figure 3c, optimized to the linear function (27a-c) in the displayed range. Most of the behavior is dominated by the leading term b_4/b_3 , and will appear linear only if an infinite number of terms are used. With five terms, the optimization routine was finding solutions where it appeared to flatten the function for \dot{h} below a certain radius, which would also require an infinite number of terms. In order to be able to fit the data for the larger range of declination angle differences with a smaller number of terms, the function for \dot{h} was made a constant (or clipped) below a threshold radius, r_h , which was then optimized.

Figure 3a also shows the result of analyzing the flyby at a starting and ending range 10 times greater than that of Figure 2 for the same set of six parameters, and the curve is lower in slope. The result appears increasingly more energy conserving, and in order to re-fit the data, the parameters would have to change, namely, b_4/b_3 , would have to increase with the range of the analysis.

In Figure 3b, the end times of each trajectory are adjusted by a point-by-point, nearly-quadratic factor to bring the data into closer agreement with Anderson's, and the adjustment factors range from 1 to 1.002. A time adjustment factor cannot be found for normal gravity (the numerical background) that would make it agree with the Anderson data, as the profile is very insensitive to

the time factors at these ranges. Therefore, in normal gravity, the time of conversion to the osculating element $V(\infty)$ is much less important than in the NGDP. The time adjustments do not have a physical interpretation, only a numerical one, which is that they are small, express the impact of the use of a limited number of terms from (26d), and again show the sensitivity of the timing and range of the analysis. Figure 3b also shows that a uniform reduction of the duration of the trajectory causes an offset without a change in shape, but has no impact on the numerical background.

The starting x-velocity of the fit in Figures 3a-b that produces zero asymptotic velocity change on the flyby is -1.42 km/s, however, the entire trajectory is different from what is expected of Newtonian gravity, shown in Figure 3d. Thus, there should be anomalous deviations from normal gravity throughout the entire trajectory even if the velocity change measured is zero at the terminal points. Note from Figure 3d that the difference in radial distance from the Earth between normal and NGDP for this example about 70 km. It is not publicly known whether it really was, and is why the model needs the full trajectory data for a proper calibration.

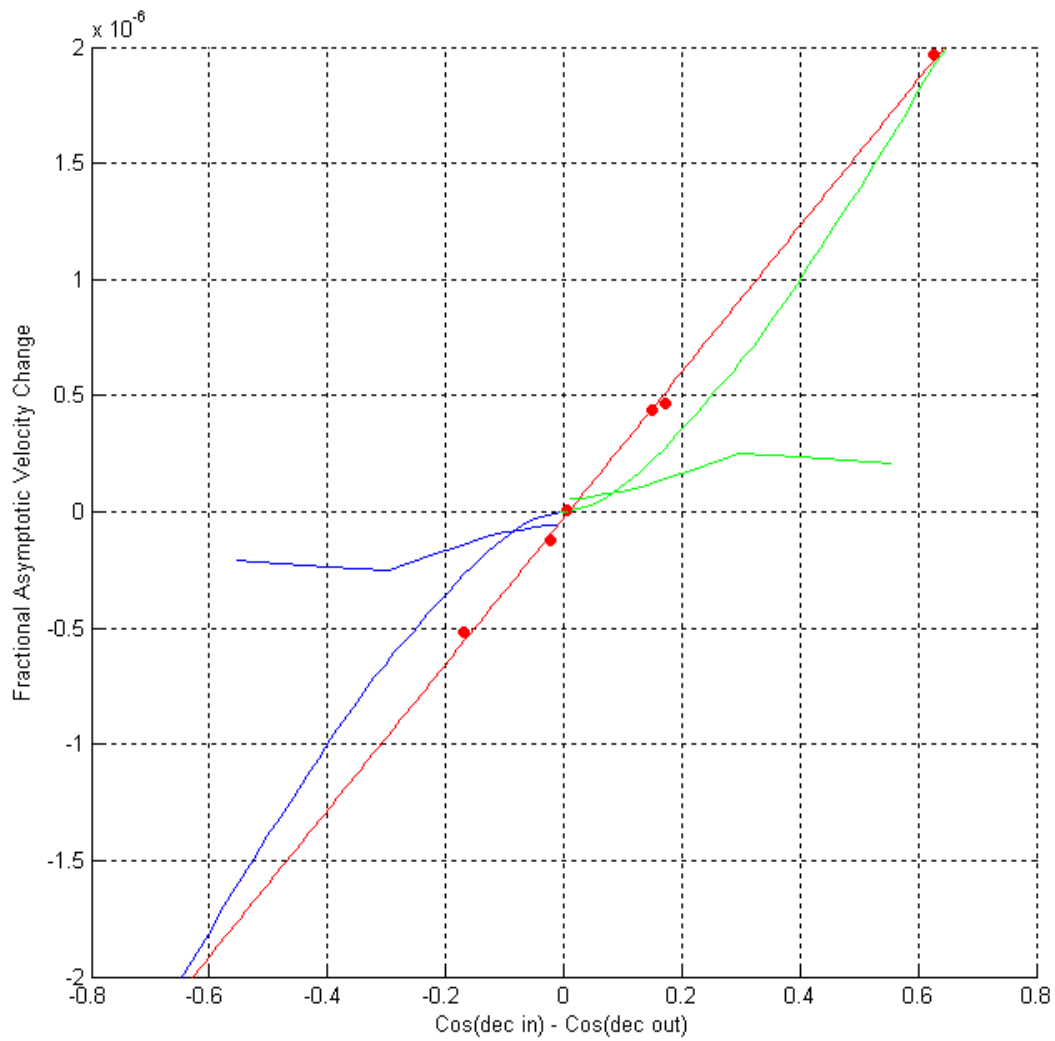


Figure 3a. Six-parameter NGDP modeling results (green and blue), against all the data of reference [34] on the flyby anomaly (red) and its reported linear fit (27a-c). Parameter values are given in the text. Equations (17a) and (26d) are used. The higher slope curves are the trajectories of Figure 2, and the lower slope curves have starting and ending range greater by a factor of 10, all other parameters fixed. The slope is going to zero with range for the same parameter set.

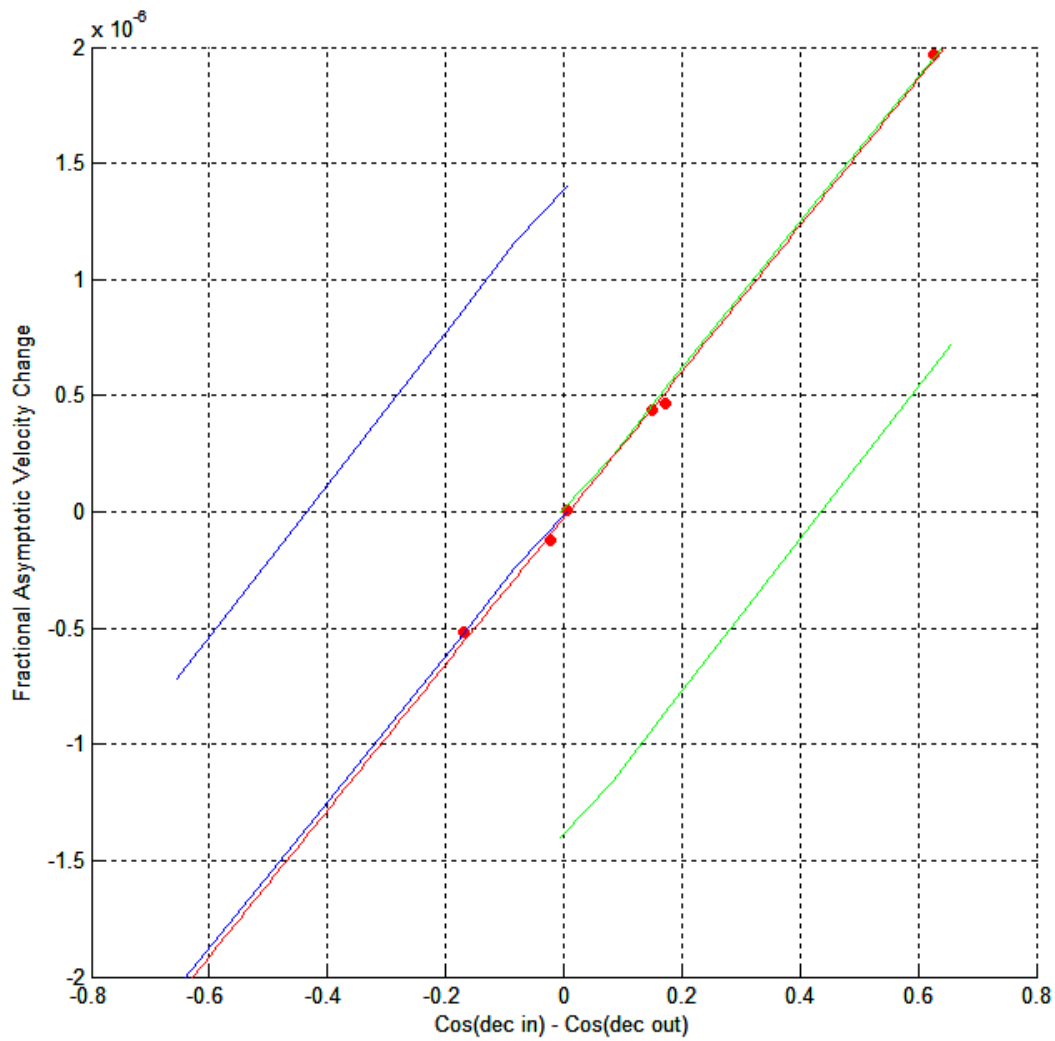


Figure 3b. Six-parameter NGDP modeling results (green and blue), against all the data of reference [34] red. The data conversion to the osculating element $V(\infty)$ occurs at the beginning and the end of trajectories, whose end times are adjusted by factors of 1 to 1.002 using a quadratic function, relative to Figure 3a. The lines offset from the red flyby data result from a uniform duration reduction of the trajectories, but not a change in shape or a change of the background.

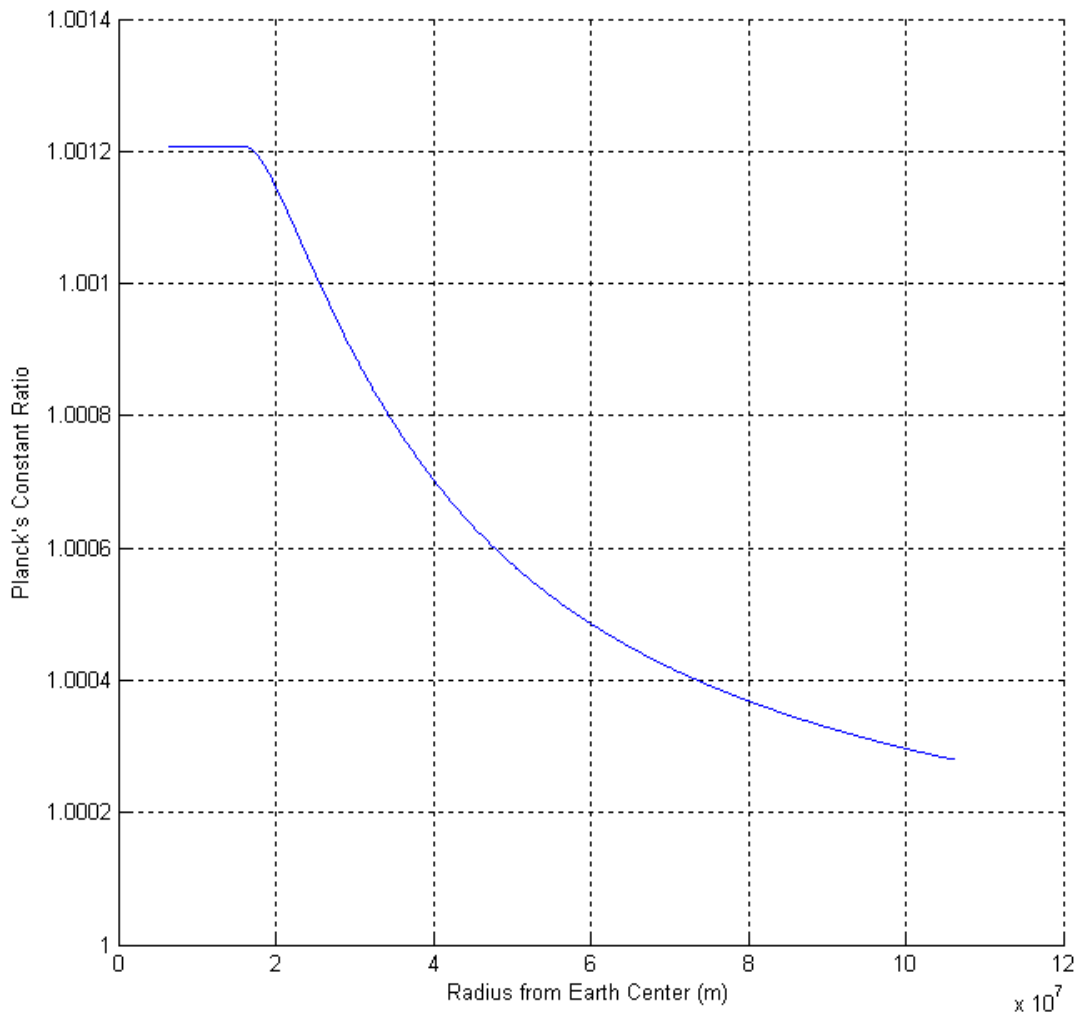


Figure 3c. Six-parameter modeling result for Planck's constant using the first five terms of (26d) (green and blue). Below $r_h = 1.628 \times 10^7$ m, the Planck's constant becomes constant (or clipped). The lowest value plotted is the radius of the Earth.

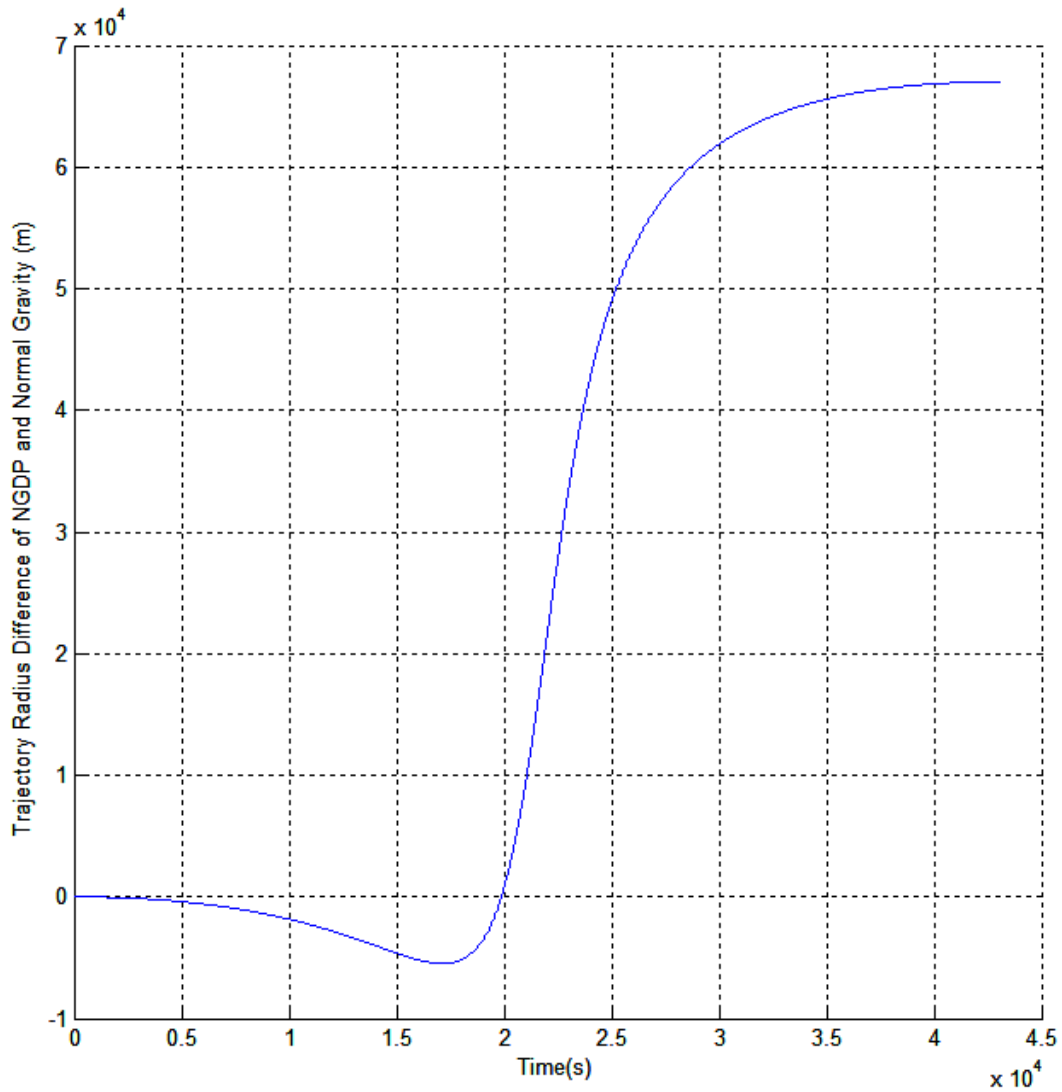


Figure 3d. For the six-parameter NGDP fit of Figure 3a, the starting x-velocity that produces an asymptotic velocity change of zero on the flyby is -1.42 km/s. The entire trajectory differs from that of Newtonian gravity, shown above as a difference in orbital radius versus time, emphasizing the orbital data as a function of time is needed to develop the true parameters, and because the energy changes inferred at finite range depend on the range of the analysis.

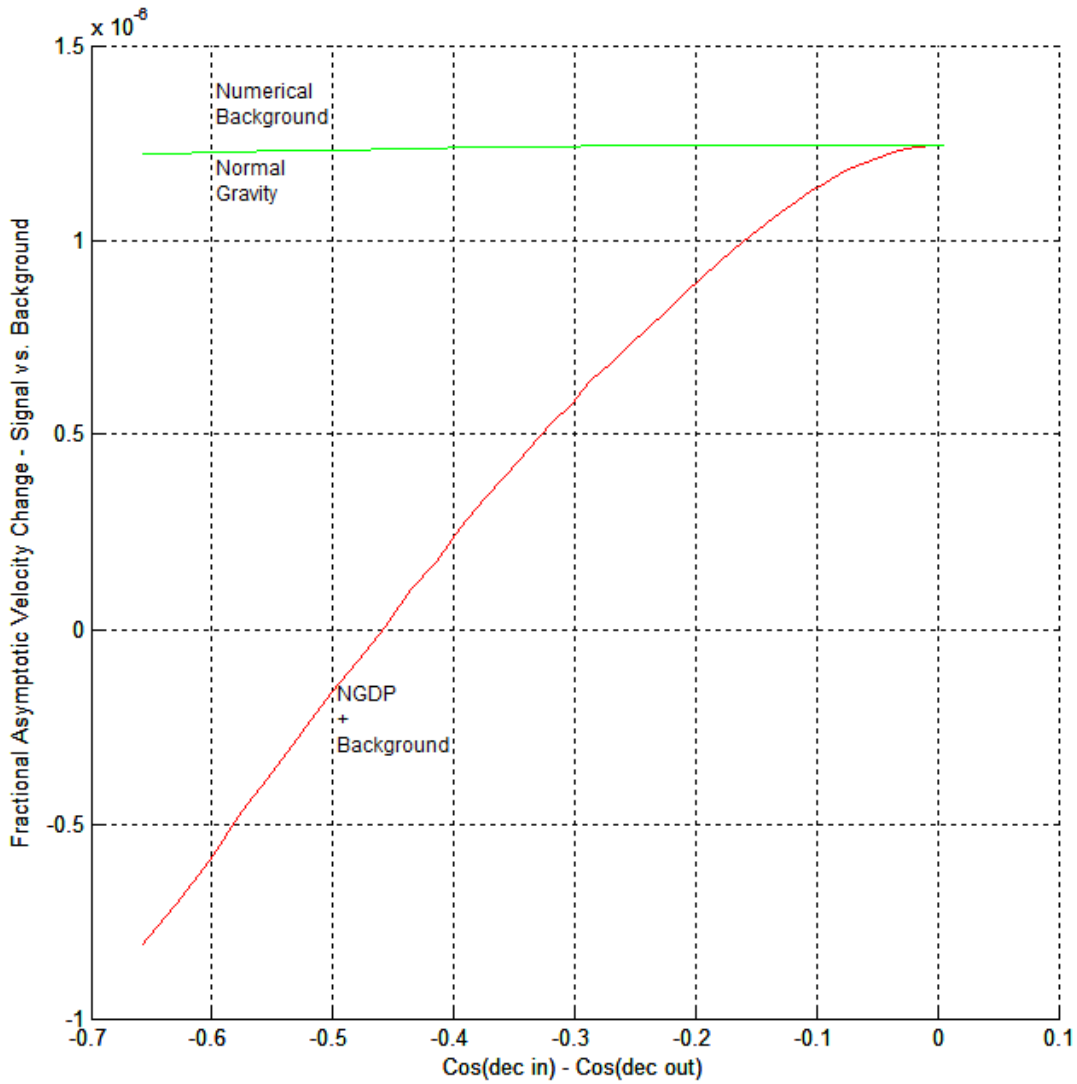


Figure 3e. The numerical background (green) of normal gravity that is subtracted from the signal+background of NGDP (red) to produce the simulation curve of Figure 3a.

In [25], a function for the variation of Planck's constant was developed from a general relativistic argument of the form,

$$\frac{\hbar(r)}{\hbar_\infty} = \left(1 - \beta_h \frac{R_S}{r}\right)^{\frac{1}{2}} = \left(1 + \frac{b_4/b_3}{r}\right)^{\frac{1}{2}} \quad (28a-b)$$

$$-\frac{b_4}{b_3} = \beta_h R_S = \beta_h \frac{2GM}{c^2}$$

where β_h is the Local Position Invariance (LPI) violation parameter, $R_S = 2GM/c^2$ is the Schwarzschild radius. Table 1 shows the extracted β_h for Earth is many orders of magnitude larger than any violation ever observed, compared to the redshift violations α_{rs} of Gravity Probe A, the GPS satellites, and the Galileo satellites. The conclusion is therefore that b_4/b_3 is independent of mass, and is representative of an effect far stronger than the redshift. The latter is discussed further in [25].

6.4 Solar System Scale Parameters: The Sun based on the Diode Experiment

The extraction of parameters for the sun is somewhat problematic. The diode experiment of [19] was essentially an Earth-bound astrophysical experiment, taking over three years to set up, collect the data, and to analyze it. Precautions were taken to remove artifacts, and divorce it from anything that might cause a systematic artifactual variation - high precision power regulation to prevent systematic drift from things like air conditioning loads in summer versus winter, and also temperature monitoring and regulation with impact on the diodes tracked and calibrated out. It was based on competing factors of Planck's constant in the tunneling exponent on which the operation of Esaki diodes is based. One factor is \hbar^2 coming from the barrier width, the other factor is \hbar^{-1} in the WKB tunneling approximation. It was the first experiment specifically devised to be sensitive to changes in \hbar - not like the high precision measurements that do not have this specific intentional feature. The signal-to-noise ratio is beyond dispute. It was correctly predicted to show a phase shift in voltage 180 degrees relative to the highly disputed radioactive decay oscillations in the literature, and when closer to the sun as the Earth orbits it, \hbar increases. There is a year-period sinusoidal signal whose analysis was published in the optics journal [19]. There is a daily signal that has gone unanalyzed, with data every 10 seconds for 941 days. The pitfall of such an experiment is that it attempts to measure the variation in a dimensioned constant. The result is potentially very important, however, because it does not attempt to extract a specific value of the constant, rather its fractional change, and because of the predicted difference in phase from the decay rates.

This is the only data of its kind, and allows an attempt at calibration of the model for the sun, for which the parameter extraction was done in [26], and is shown in Table 1. The peak-to-peak swing $\delta\hbar/\hbar$ is reported to be 21 ppm [19]. These diode measurements show variations higher than that of NIST measurements of Planck's constant with a precision of $\sim 10^{-8}$ [35], where the latter measurements are made at the Earth's surface, but were not specifically designed to be sensitive to variations in Planck's constant, such as the diode experiment was with intentionally competing factors of \hbar .

A notable result shown in Table 1 is that the b_4/b_3 of the Earth based on the flyby is about the same as that extracted from the uncertainty of the NIST measurement of \hbar used as if it was equal to the swing $\delta\hbar/\hbar$, and both are less than the sun's by several orders based on the diodes. One might conclude that b_4/b_3 increases with M , but it will be explained why this is not so in the discussion, and it is essentially because it leads to problems with the orbits of a Hulse-Taylor-like binary, the Earth, and Mercury, the latter being rectifiable even for the diode swings with more terms in the series, but not the former.

Table 1 also shows that the β_h values from the diode experiment greatly exceed the redshift violation parameters α_{rs} of Gravity Probe A, the GPS satellites, and the Galileo satellites, where again it is concluded that b_4/b_3 is independent of mass, and is representative of an effect far stronger than the redshift.

The gain in the diode experiment may be different than was computed in [19], where,

$$I = C(h)V \exp\left(-\frac{8\pi}{3} x_{bo} \frac{h}{h_o^2} \sqrt{2m_e e (V_b(h) - V)}\right) \quad (29a-b)$$

$$\delta V / V = f \cdot \delta h / h$$

If one assumes that the only influence on a change in \hbar is the change itself in the exponent, and the diode barrier width $x_b = x_{bo}(\hbar/\hbar_o)^2$, and nothing else, one finds the result of [19] that the gain in constant current mode was $f = -40.8$. However, if the length can change with \hbar in all of the rest of the metrology (resistors, diodes, meters, sources) encapsulated in $C(h)$, and also the built-in voltage of the diode $V_b(h)$, then the gain will be different than what was computed. The true diode characteristics (I-V curves) were also not used, only the basic physical argument. The metrology of such an experiment needs much deeper analysis, as there are many neglected terms contributing to the gain.

Near the sun surface, the $\Delta\hbar/h_\infty$ extracted would also be unphysically high. As will be explained, this is rectified by the use of more terms in the expansion of (26d) to reduce it, without impacting the results at greater distances, or to clip it, as was done for the flyby.

7. Discussion and Impact on Gravitational Radiation

The model presented that seems to fit the flyby anomaly data fairly well is truly non-energy conserving. There is no additional field in the model for gravity to exchange energy with causing it to simply appear that energy was not conserved because the exchange is unaccounted for in the motion of the spacecraft. The starting point for the development in this paper could not be derived from an energy-conserving field theory [26]. In this model, W is conserved, the frequency of the dominant path. It has been recently confirmed that the flyby anomaly observation has gone unresolved to this day, while also the very few satellites since that have been examined did not exhibit the anomaly [36]. A detailed modeling effort using the actual orbital data as a function of time, if it could be made available, would be worthwhile to undertake. The effects of the model here could be investigated, and also of a field-based model, where the exchange of energy is possible, both with and without a field representative of Planck's constant that was formatively derived in [26].

Body	Obs.	$\delta\hbar/\hbar^{(2)}$	M (kg)	b_4/b_3 (m) ⁽²⁾	Ω_{PE} ⁽⁸⁾	Ω_{PM} ⁽⁹⁾	R (m) ⁽⁴⁾	β_h ^(5,3)	$\Delta\hbar(R)/h_\infty$	Ref.
Earth	Flyby		5.97×10^{24}	6×10^4			6.38×10^6	-6.67×10^6	4.69×10^{-3}	[34]
Sun	Diode	21×10^{-6}	1.99×10^{30}	1.62×10^8	-1411	-3751	6.96×10^8	-5.43×10^4	1.09×10^{-1}	[19],[26]
Sun/Earth ⁽¹⁾			3.3×10^5	2.70×10^3						
Sun	NIST ⁽¹¹⁾	$< 10^{-8}$	1.99×10^{30}	$< 7.70 \times 10^4$	-0.996	-2.599	6.96×10^8	$< -26.1 $	$< 5.53 \times 10^{-5}$	[35],[26]
Sun	Small ⁽⁷⁾		1.99×10^{30}	100	-0.001	-0.0034				
1.4×Sun ⁽¹⁰⁾	Binary			$\pm 4.5 \times 10^5$						[38]
	Satellite							α_{rs} ^(6,3)		
	Galileo							$4.5 \pm 3.1 \times 10^{-5}$		[12]
	GP- A							1.4×10^{-4}		[12]
	GPS							$\beta_h < 0.007 $		[10],[11]

Table 1. Use of equations (17a), (26), and (28a-b) to extract parameters for Planck's constant using the leading order one-parameter fit. The reference for the data used in the calculation is indicated in the last column. Note the b_4/b_3 values extracted for the sun are greater than the Earth's.

¹ Ratios are those of sun-Diode/Earth-Flyby

² Procedure to extract b_4/b_3 from the swing $\delta\hbar/h$ is described in [26]. The evaluation radius is the sun-Earth orbit 1 AU.

³ Compare the redshift violation parameter α_{rs} to Planck's constant LPI violation parameter β_h .

⁴ Surface radius of the body.

⁵ Inequalities refer to absolute values. $\beta_h = (b_4/b_3)/R_S$ is used to calculate the top three table elements. The others are from literature.

⁶ GR could explain clock frequency shifts up to this redshift factor $\Delta f/f = (1 + \alpha_{rs})\Delta U/c^2$.

⁷ Investigating the "small value" of 100 m, evidencing that the extracted value for the sun must fall off with range much faster.

⁸ Perihelion precession of Earth in arcseconds per orbital period.

⁹ Perihelion precession of Mercury in arcseconds per orbital period. For comparison the GR result for this is +0.104 arcseconds per period.

¹⁰ Value needed to alter the rate of orbital period change by $\mp 0.13\%$ of a 1.4 solar mass Hulse-Taylor-like binary.

¹¹ The uncertainty of the NIST measurement of h is used as if equal to the swing $\delta\hbar/h$ at the Earth caused by the Sun's h field.

Such actions for interacting fields could be of the form (I1a-e), or

$$S_N = \int \left\{ -\frac{1}{8G_o\pi} \xi \eta^{\mu\nu} \partial_\mu \varphi \partial_\nu \varphi + \rho \varphi + \frac{(\hbar_o \psi)^2}{2} \eta^{\mu\nu} \partial_\mu \psi \partial_\nu \psi + \frac{(\hbar_o \psi)^2}{2} \frac{w}{\xi} \eta^{\mu\nu} \partial_\mu \xi \partial_\nu \xi + \lambda \xi \psi \varphi \right\} d^4 x$$

$$\hbar = \hbar_o \psi$$

$$G = G_o / \xi$$

(31a-c)

or, considering actions of the form of (32) where \hbar may or may not have time dependence, and the dynamical term for Planck's constant may or may not appear,

$$\int dt \frac{L_c(x(t), \dot{x}(t))}{\hbar(x(t), t)} \rightarrow \int \left\{ \frac{\frac{c^4}{16G\pi} R + \frac{(\hbar_o \psi)^2}{2} g^{\mu\nu} \nabla_\mu \psi \nabla_\nu \psi + L_m \{ \hbar \}}{\hbar_o \psi} \right\} \sqrt{-g} d^4 x \quad (32)$$

Equation (31a) is a special relativistic version in flat spacetime, with gravitational potential φ . There are many such couplings and combinations that may be tried. Variations in c or c^4 might be added, per (I1a-e) and [31-32]. Equation (32) is motivated by the path integral result.

The couplings of the fields would have to be orchestrated in a way that a test mass can acquire additional velocity in an energy conserving manner, where for example, G falls in time or position while the spacecraft is passing Earth, leading to a higher than expected final velocity, because it took less energy to escape the Earth compared to when the test mass entered. As for positional dependences of G alone with no time dependence, they would have to be asymmetric about the Earth in some way to appear non-conservative, and while that is possible to arrange mathematically, it seems physically unlikely since the asymmetric arrangement must generate just the right boosts for all the different satellite orbits. That leaves a time variation as a possibility that would have to be exquisitely timed in order to coincide with the when and how of all six satellite flybys, and so is also unlikely.

That leaves artifacts. Since the very few flybys since the Anderson paper [34] have not shown the anomaly [36], it may be that an undiscovered systematic problem was corrected in the tracking improvements since 2008, and whether that is so is an unknown and may remain so. It may not be sufficient to simply analyze the asymptotic velocity differences, rather, the data of the entire trajectory should be examined because it may show other anomalies. Such data needs to be made available. The flyby anomaly is simply not something that is routinely observed every time, for example, the Juno spacecraft passing near Earth in 2013 [38].

The value of K and the form found empirically for it shown in (27a) resembles twice the Doppler shift from the velocity of the rotating Earth, multiplied by an angular dependence. The derivation in [37] based on the transverse Doppler effect results in Equation (27a), the change in velocity is concluded to be an artifact, and one wonders why the flyby anomaly is still listed as an unsolved problem in physics in light of this result – the theory of [37] has not been directly proven by a detailed analysis of the flyby data throughout the entire trajectory, however. The models developed here do not address the empirically determined constant involving the Earth rotation, which may be fortuitous.

The model developed here must be calibrated so as to not be at odds with well-observed phenomena. Recall the path integral derivation was for mild gradients in \hbar , both in the approximate basis used, and also due to the findings in [25] on the Schrödinger equation for when the gradient is small, that planewave solutions for free particles hold approximately, and the Ehrenfest theorem relating the time derivative of the expectation value of position to the momentum is exactly reproduced. The latter is maintained when $b_4/b_3 / r \ll 1$.

Consider the impact of the flyby parameters on the moon's orbit, where at the radius of the lunar-Earth orbit, $\Delta\hbar/h_\infty = 8.269 \times 10^{-5}$. A numerical calculation performed for the moon's orbit about a fixed-position Earth, using (17a) and the six-parameter fit resulted in small changes that were computationally challenging. The apogee would increase by about 94 km compared to normal gravity, when the orbit is begun at the same perigee and orbital speed as is measured. The actual perigee is known to vary over a range of about 14,000 km, and the apogee over 2700 km, so if the effect was active, this aspect of it may be masked. The apogee increase is insensitive to the time increment used in the simulation, while the orbital radius change with time is. The orbital radius at apogee falls by -3700 m/yr at 5000 timesteps per orbital period, -926 m/yr at 20,000 timesteps per period, and -308 m/yr at 60,000 timesteps per period, converging as $-2 \times 10^7 / N^{1.002}$ m/yr, where N is the number of time divisions per orbital period. The numerical solution is

approaching zero. These calculations are pushing the limits of the computational resources available to the author at the time of this writing. Lunar Laser Ranging puts the moon's orbit to be increasing in radius by +3 cm/yr. The 6-parameter fit also predicts an additional -201 arcsecond/period apsidal precession, small compared to the observed one, $\sim +11,000$ arcsecond/period. If these are not numerical artifacts, the decay function (26e) could be utilized. Putting $a \sim s \sim 10^8$ m rectifies all issues with the moon while not affecting the ability to fit the flyby, and without introducing sharp transitions in the function for \dot{h} .

For the sun-to-Earth radius based on the diode experiment, Gravity Probe A, and the Galileo satellites, at 1 AU $\Delta\dot{h}/h_\infty \geq 5.41 \times 10^{-4}$, and the extracted value $\Delta\dot{h}/h_\infty \geq 0.11$ or higher at the sun surface (Table 1) would negate fusion - however, the approximation of the mild gradient is now breaking down. The b_4/b_3 value extracted from it for the sun would affect the orbit of the Earth and Mercury. A numerical study performed for the orbits shows that if the diode parameter values of Table 1 are used for the sun along with only the leading term of (28), the apsidal precession becomes large and negative, but that is what has to happen to maintain the 21 ppm swing $\delta\dot{h}/\dot{h}$ reported in the diode experiment, and adding terms to lower the gradient there will reduce the predicted variation, taking it out of agreement. The precession and the measured reported variation in $\delta\dot{h}/\dot{h}$ are boundary conditions in opposition, and the problem cannot be solved this way, but could if the variation were just shown to be smaller from neglected gain terms. The diode data therefore remains as a qualitative example of a dimensioned constant that might be varying, awaiting more analysis, especially of the measurement system for superimposed signals or unaccounted-for amplification factors. The data can be made available by the author of [19].

Table 1 shows that if the swing in $\delta\dot{h}/\dot{h}$ at the Earth over the sun-Earth orbit was not 21 ppm, but set as if 1×10^{-8} per the precision of the NIST measurements or the flyby b_4/b_3 value, the $\Delta\dot{h}/h_\infty$ at the sun surface $\sim 10^{-5}$, so there is no fusion problem, but the precessions are still too high.

It will be illustrated how the use of additional terms can rectify some problems while not disturbing other results. Assume that the 21 ppm swing of the diode test is real, and must be maintained in the model. The issue at the sun surface a distance from its center R with the overly large change in \dot{h} is rectified through the use of the $l=1$ term in (26d) with $B_1 = -7.85 \times 10^{16}$ km³. With this, the $\Delta\dot{h}/h_\infty$ at the sun surface goes to zero, yet the extra term is too small to alter the 21 ppm variation at the Earth's orbital radius. The problem with the precession of the orbit of Mercury can also be resolved by adding another term, and generally problems "interior" to the leading term are fixed with more terms. The problem with the predicted orbit of the Earth is not resolved if the swing remains 21 ppm, of course.

If the diode data were used at face-value, it might have been concluded that the effects increase proportionally with mass. That conclusion cannot be made at this time. An effect increasing proportionally with mass may have a detectable impact on systems like the Hulse-Taylor binary pulsar, and for that case, the evolution through the radiation of gravitational waves matches the predictions of general relativity to within 0.13% [38]. A system may be found in the future where it is not as well described.

An orbit for a Hulse-Taylor-like binary for a highly-exaggerated effect is computed using only the model of this paper and the parameter extracted from the diode experiment, shown in Figures 4-5. While the orbital period does not change with time, the orbital period increases from 8.1 hours for the Newtonian calculation shown in Figure 4, to 11.8 hours in this papers model, with a pronounced negative apsidal precession shown in Figure 5, for all other parameters fixed.

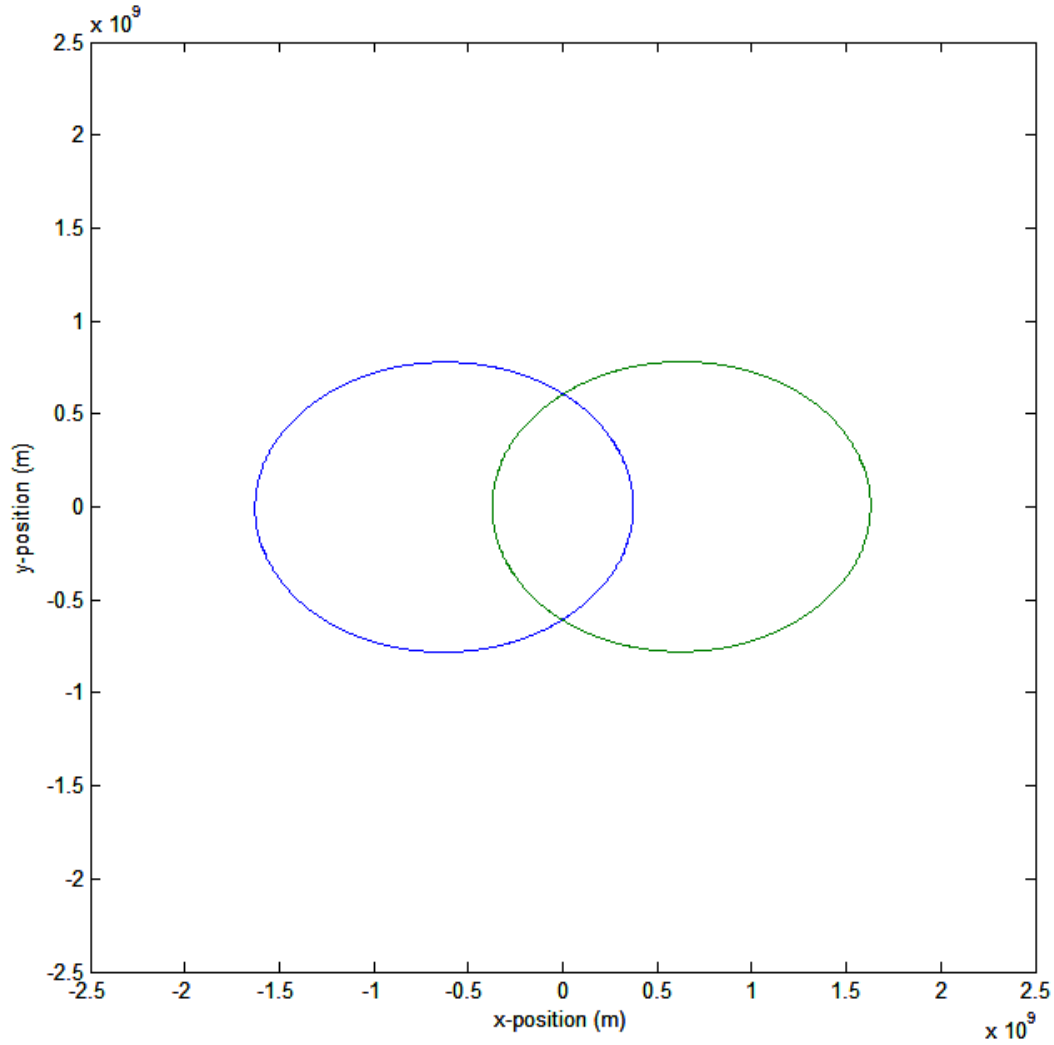


Figure 4. Use of Equations (17a) and (26d-e) to numerically compute the orbit of a Hulse-Taylor-like binary. Each mass is 1.4 solar masses placed at 746,000 km at periastron and launched in opposite directions vertically at 450 km/s. The Newtonian result is shown and has a period of 8.1 hours.

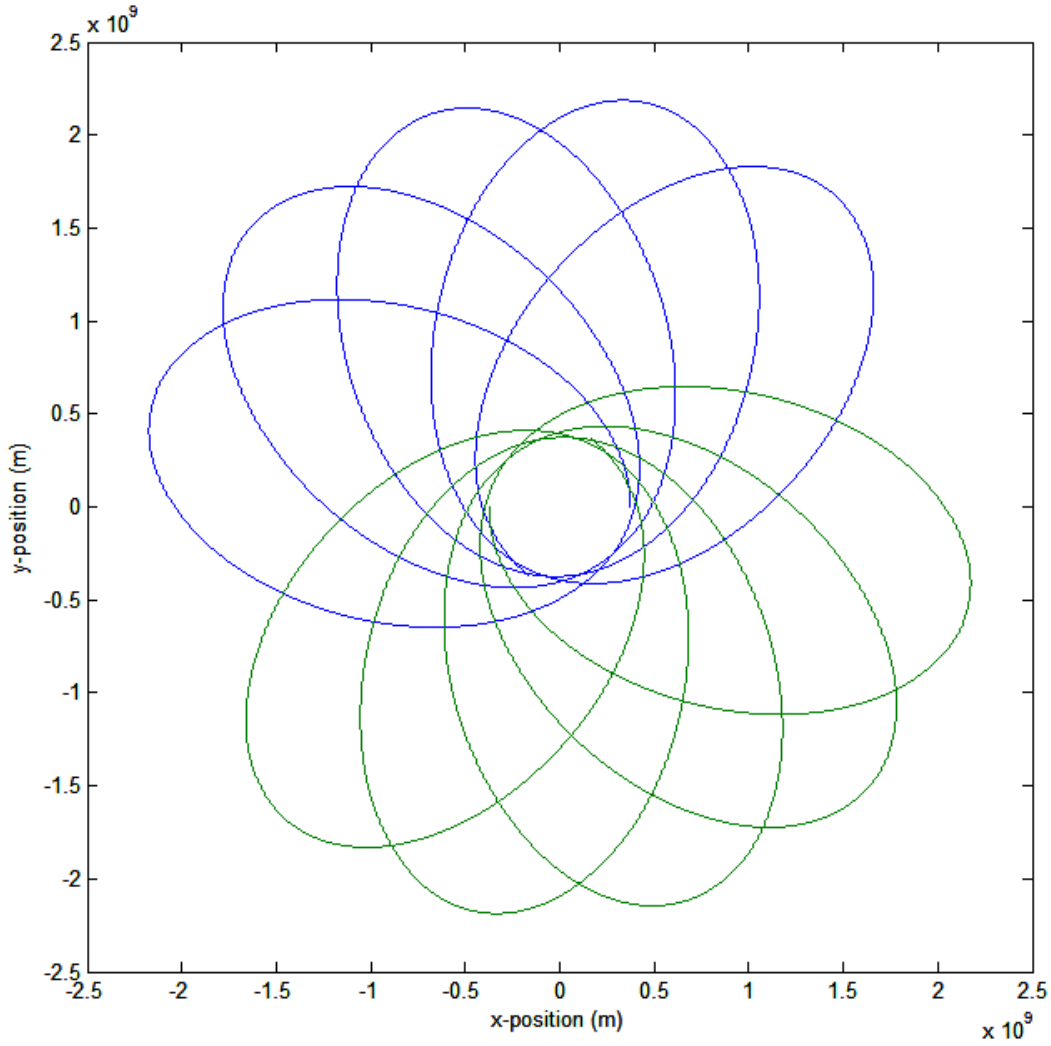


Figure 5. Use of Equations (17a) and (26d-e) to numerically compute the orbit of a Hulse-Taylor-like binary for NGDP. Each mass is 1.4 solar masses placed at 746,000 km at periastron and launched in opposite directions vertically at 450 km/s. Using the diode b_4/b_3 value for the sun from Table 1 multiplied by 1.4, the resulting orbit is shown, and now has a period of 11.78 hours, and a negative apsidal precession (opposite the orbital direction) of -104,000 arcseconds per period.

For the example of the binary orbit being considered, its rate of period reduction by emission of gravitational waves should be per [39] with $e=0.62$ and Equation (33),

$$\dot{P}_{GW} = -\frac{192\pi G^{5/3}}{5c^5} \left(\frac{P}{2\pi}\right)^{-5/3} (1-e^2)^{-7/2} \left(1 + \frac{73}{24}e^2 + \frac{37}{96}e^4\right) \frac{m_p m_c}{(m_p + m_c)^{-1/3}} \quad (33)$$

the rate of period reduction is -2.25×10^{-12} s/s for the binary of normal gravity, and -1.20×10^{-12} s/s for the NGDP calibrated with the diode data multiplied by 1.4. Calibrated with the flyby parameters (or assumed NIST parameters), the precession of the periastron is predicted to be about -13 deg/year. In either case, it was concluded that there is no change in the orbital period as a function of time. A reduction in the period as a function of time was actually computed, but this period reduction rate was linear in the time increment of the numerical simulation tending towards zero, suggesting a numerical artifact, while the overall shape and precession of the orbit was insensitive to the time increment.

Therefore, the impact of such an additional force on the radiation of gravitational waves is to cause a negative apsidal precession that would not normally occur, and to have larger than expected orbital periods, resulting in slower than expected period decrease rate due to decreased gravitational wave emission. Using Equation (33) and the leading term only in the numerical simulation of the binary under discussion, a $\pm 0.13\%$ discrepancy in the rate of period reduction could be explained with a $b_4/b_3 = \mp 4.5 \times 10^5$ m, a surprisingly large number, and an apsidal precession results of -90.44 deg/year, too large, and is just further evidence that the parameter cannot be this large, or must decay with range faster than is modeled.

The diode scenario considered for the sun in Table 1 all has upper-limit b_4/b_3 values significantly higher than that extracted for the Earth, but it is concluded that the parameter is not mass dependent owing to the problems that arise if it were, and because the derivation of it in [26] does not involve mass. Since it is not in direct proportion to mass, which the definition of the parameter β_h depends on, this explains the high values extracted for it. The value of $b_4/b_3 = 60,000$ m is consistent with the flybys, but to be consistent with the observed orbits of the planets, possibly the moon, and Hulse-Taylor binary, must be less than this, and/or decay faster with range than $1/r$. Additional terms in the function for Planck's constant are available for the latter, but, to extract the parameters more meaningfully, the entire trajectory really needs to be fit, and that data is presently not available.

The constant b_4/b_3 value is arrived at from fitting, and whose value cannot be explained anymore than that of Planck's constant, or any other. This constant arises in a classical field theory for the vacuum, whose center is made coincident with large masses, but is independent of their mass. It is associated with the leading term, and is the active term when $b_4/b_3 \ll r$. When this condition is not satisfied at closer ranges, other terms become important in reducing the $\Delta\hbar/h_\infty$.

In [25], it was found that there was little simpatico between the Ehrenfest theorems and classical mechanics for a position dependent \hbar in the frequency-conserving Schrödinger equation, and Equation (14b) clarifies why this is so - Newtonian dynamics changes.

Other accepted non-energy conserving events were, or are at work, such as the Big Bang, and the accelerated expansion of the universe driven by the cosmological constant. The additional term in the Friedmann equation (24) from a spatial variation in \hbar may be relatable to the latter, and while total energy in the universe is still not conserved in the expansion, total frequency would be. An alternative path, a starting point, to an explanation of the nature of dark matter is offered – a spatial variation in \hbar causes a macroscopic force assisting the dark matter in holding galaxies together, while suppressing the normal known forces dependent on \hbar , and unable to quantum

mechanically interact, it cannot lose energy (or frequency) by normal mechanisms, and remains dark.

8. Conclusions

A modified form of the path integral for a position dependent Planck's constant is derived for the limit of a mild spatial gradient. The variations in Planck's constant are not treated as an energy conserving dynamical field here – that may be found in [26]. A path termed as “dominant” is identified that makes the integral in the exponent stationary. Modifications to Newton's Laws, Newtonian gravity, and the Friedmann equation are found. An initial attempt is made to address anomalous energy changes in satellite flyby orbits noted by the Jet Propulsion Laboratory, and a good, quantitative agreement is found for the energy changes, but requires detailed orbital data as a function of time, and greater computational precision than was available at the time of this writing to do better. The anomaly is here explained to stem from a combination of the lack of energy conservation at close range, and the inability to collect and analyze data at true infinite range. The detailed trajectory data for the whole flyby would need to be brought out of archive, and then also formatted so that it can be used by independent investigators, if the information still even exists [36]. The β_h parameter values extracted for the Earth for the flybys are very large, as are those extracted for the sun from the diode experiment, neither of which are experiments with clocks and light. The Gravity Probe A, GPS, and the Galileo satellite redshift violation parameters α_{rs} and β_h are orders lower, are three experiments with clocks, and it was rationalized that a variation in \hbar may be undetectable with clock and light measurements at different altitudes if total frequency is conserved [25]. It is concluded the leading parameter b_4/b_3 does not depend on mass and describes an effect much stronger than the redshift [25]. The high b_4/b_3 parameter values extracted for the sun from the diode experiment cause a number of orbital problems, and so it is concluded the diode experiment needs repeating by independents, and more in-depth analysis of what its measured variations mean. The parameter $b_4/b_3 \leq 60,000$ m, and/or \hbar must decay with range faster than $1/r$.

Methods to test the model's concrete predictions would be: 1) the intentional set up and analysis of the entire trajectories of satellite flyby orbits that maximize the effect; 2) monitoring of gravitational wave emission of binary mergers that do not match expected theory, with longer periods than the masses involved predict, and slower orbital period reductions; 3) observation of unexpected negative apsidal precession in bound orbits.

9. Acknowledgements

Many thanks to Dr. Richard Hutchin and Optical Physics Company for supporting this work, and to Dr. Luis Acedo Rodríguez of Instituto de Matemática Multidisciplinar, Universitat Politècnica de València for extremely helpful discussions, classical perturbation theory insights, and other careful examinations.

10. References

[1] P. A. M. Dirac, A New Basis for Cosmology. Proc. Royal Soc. London A 165 (921) 199–208 (1938)

- [2] A. P. Meshik, The Workings of an Ancient Nuclear Reactor, *Scientific American*, January 26, (2009)
- [3] J.-P. Uzan and B. Leclercq, *The Natural Laws of the Universe: Understanding Fundamental Constants*. Springer Science & Business Media, (2010)
- [4] J. K. Webb, M. T. Murphy, V. V. Flambaum, V. A. Dzuba, J. D. Barrow, C. W. Churchill, and A. M. Wolfe, Further evidence for cosmological evolution of the fine structure constant. *Phys. Rev. Lett.* 87(9), 091301 (2001)
- [5] Sze-Shiang Feng, Mu-Lin Yan, Implication of Spatial and Temporal Variations of the Fine-Structure Constant, *Int. J. Theor. Phys.* 55, 1049–1083 (2016)
- [6] L. Kraisselburd, S. J. Landau, and C. Simeone, Variation of the fine-structure constant: an update of statistical analyses with recent data. *Astronomy & Astrophysics* 557, (2013)
- [7] G. Mangano, F. Lizzi, and A. Porzio, Inconstant Planck's constant, *Int. J. of Mod. Phys. A* 30(34) (2015) 1550209
- [8] Maurice A. de Gosson, Mixed Quantum States with Variable Planck's Constant, *Physics Letters A* Volume 381, Issue 36, Pages 3033-303 (2017)
- [9] Jean-Philippe Uzan, The fundamental constants and their variation: observational and theoretical status, *Reviews of Modern Physics*, 75, 403-455 (2003)
- [10] J. Kentosh and M. Mohageg, Global positioning system test of the local position invariance of Planck's constant, *Phys. Rev. Lett.* 108(11) (2012) 110801
- [11] J. Kentosh and M. Mohageg, Testing the local position invariance of Planck's constant in general relativity. *Physics Essays* 28(2), 286–289 (2015)
- [12] Sven Herrmann, Felix Finke, Martin Lulf, Olga Kichakova, Dirk Puetzfeld, Daniela Knickmann, Meike List, Benny Rievers, Gabriele Giorgi, Christoph Günther, Hansjörg Dittus, Roberto Prieto-Cerdeira, Florian Dilssner, Francisco Gonzalez, Erik Schönemann, Javier Ventura-Traveset, and Claus Lämmerzahl, Test of the Gravitational Redshift with Galileo Satellites in an Eccentric Orbit *Phys. Rev. Lett.* 121, 231102 (2018)
- [13] Ellis, K.J., The Effective Half-Life of a Broad Beam $^{238}\text{Pu}/\text{Be}$ Total Body Neutron Radiator. *Physics in Medicine and Biology*, 35, 1079-1088(1990)
<http://dx.doi.org/10.1088/0031-9155/35/8/004>
- [14] Falkenberg, E.D., Radioactive Decay Caused by Neutrinos? *Apeiron*, 8, 32-45(2001)
- [15] Alburger, D.E., Harbottle, G. and Norton, E.F., Half-Life of ^{32}Si . *Earth and Planetary Science Letters*, 78, 168-176(1986). [http://dx.doi.org/10.1016/0012-821X\(86\)90058-0](http://dx.doi.org/10.1016/0012-821X(86)90058-0)

- [16] Jenkins, J.H., et al., Analysis of Experiments Exhibiting Time Varying Nuclear Decay Rates: Systematic Effects or New Physics?(2011) <http://arxiv.org/abs/1106.1678>
- [17] Parkhomov, A.G., Researches of Alpha and Beta Radioactivity at Long-Term Observations.(2010) <http://arxiv.org/abs/1004.1761>
- [18] Siegert, H., Schrader, H. and Schötzig, U., Half-Life Measurements of Europium Radionuclides and the Long-Term Stability of Detectors. Applied Radiation and Isotopes, 49, 1397(1998).[http://dx.doi.org/10.1016/S0969-8043\(97\)10082-3](http://dx.doi.org/10.1016/S0969-8043(97)10082-3)
- [19] Richard A. Hutchin, Experimental Evidence for Variability in Planck's Constant, Optics and Photonics Journal, 6, 124-137 (2016)
- [20] Cooper, P.S. (2008) Searching for Modifications to the Exponential Radioactive Decay Law with the Cassini Spacecraft. <http://arxiv.org/abs/0809.4248>
- [21] Norman, E.B., Browne, E., Chan, Y.D., Goldman, I.D., Larimer, R.-M., Lesko, K.T., Nelson, M., Wietfeldt, F.E. and Zliten, I., Half-Life of ^{44}Ti . Physical Review C, 57 (1998)
- [22] E. N. Alexeyev, Ju. M. Gavriljuk, A. M. Gangapshev, A. M. Gezhaev, V. V. Kazalov, V. V. Kuzminov, S. I. Panasenko, S. S. Ratkevich, S. P. Yakimenko, Experimental test of the time stability of the half-life of alpha-decay Po-214 nuclei, (2011) <https://arxiv.org/abs/1112.4362>
- [23] Eric B. Norman, Additional experimental evidence against a solar influence on nuclear decay rates (2012) <https://arxiv.org/abs/1208.4357>
- [24] Karsten Kossert, Ole Nähle, Disproof of solar influence on the decay rates of $^{90}\text{Sr}/^{90}\text{Y}$ (2014) <https://arxiv.org/abs/1407.2493>
- [25] Rand Dannenberg, Position Dependent Planck's Constant in a Frequency-Conserving Schrödinger Equation, (2019). <https://arxiv.org/abs/1812.02325>
- [26] Rand Dannenberg, Planck's Constant as a Dynamical Field, (2019).<https://arxiv.org/abs/1812.02325>
- [27] J.D.Bekenstein, Fine-structure constant: Is it really a constant, Phys.Rev.D25,1527(1982)
- [28] J.D. Bekenstein, Fine-structure constant variability, equivalence principle and cosmology, Phys. Rev. D66, 123514 (2002)
- [29] C. Wetterich, Naturalness of exponential cosmological potentials and the cosmological constant problem (2018), preprint <https://arxiv.org/abs/0801.3208>
- [30] C. Wetterich, Cosmological inflation. (2013) preprint <https://arxiv.org/abs/1303.4700>

- [31] A. Albrecht; J. Magueijo, A time varying speed of light as a solution to cosmological puzzles. Phys. Rev. D59 (4): 043516 (1999)
- [32] J.D. Barrow, Cosmologies with varying light-speed. Physical Review D. 59 (4): 043515 (1998)
- [33] Andrew Liddle, Introduction to Modern Cosmology, Second Edition, John Wiley & Sons Ltd, John Wiley & Sons Ltd, The Atrium, Southern Gate, Chichester, West Sussex PO19 8SQ, England (2003)
- [34] John D. Anderson, James K. Campbell, John E. Ekelund, Jordan Ellis, and James F. Jordan, Anomalous Orbital-Energy Changes Observed During Spacecraft Flybys of Earth, Phys Rev Letters, 100, 091102. (2008)
- [35] Schlamminger, S., Haddad, D., Seifert, F., Chao, L. S., Newell, D. B., Liu, R., Steiner, R. L., Pratt, J. R., "Determination of the Planck constant using a watt balance with a superconducting magnet system at the National Institute of Standards and Technology". Metrologia. 51 (2): S15. (2014)
- [36] Private communication with Dr. Slava Turyshev, Structure of the Universe Research Group, Caltech/NASA Jet Propulsion Laboratory, Pasadena, CA, February 2019
- [37] Jean Paul Mbelek, Special relativity may account for the spacecraft flyby anomalies (2009) <https://arxiv.org/ftp/arxiv/papers/0809/0809.1888.pdf>
- [38] Paul F. Thompson, Matthew Abrahamson, Reconstruction of the Earth Flyby of the Juno Spacecraft (2014).
- [39] Joel M. Weisberg, Joseph H. Taylor, The Relativistic Binary Pulsar B1913+16: Thirty Years of Observations and Analysis, Binary Radio Pulsars ASP Conference Series, Vol. 328, (2005)
- [40] L. Acedo, P. Piqueras and J. A. Morano, A possible flyby anomaly for Juno at Jupiter, (2017) <https://arxiv.org/pdf/1711.08893.pdf>
- [41] J. W. Moffat, Superluminary universe: A Possible solution to the initial value problem in cosmology Int.J.Mod.Phys. D2 351-366 (1993)
- [42] J. W. Moffat, Variable Speed of Light Cosmology, Primordial Fluctuations and Gravitational Waves. Eur. Phys. J. C 76:13 (2016)